DEUTSCHES ELEKTRONEN – SYNCHROTRON

DESY 93-028
March 1993

Unitarity Corrections to the Lipatov Pomeron and the Four-Gluon Operator in Deep Inelastic Scattering in QCD

J. Bartels

II. Institut für Theoretische Physik, Universität Hamburg

ISSN 0418-9833

NOTKESTRASSE 85 · D-2000 HAMBURG 52

To be sure that your preprints are promptly included in the
HIGH ENERGY PHYSICS INDEX,
send them to (if possible by air mail):

DESY **Bibliothek** **Notkestraße 85** **W-2000 Hamburg 52** **Germany**	**DESY-IfH** **Bibliothek** **Platanenallee 6** **O-1615 Zeuthen** **Germany**

DESY 93-028
March 1993

ISSN 0418-9833

Unitarity Corrections to the Lipatov Pomeron and the Four-Gluon Operator in Deep Inelastic Scattering in QCD

J.Bartels

II. Institut für Theoretische Physik, Universität Hamburg,

Abstract: Starting from a four-gluon partial-wave amplitude which provides the first unitarity corrections to the Lipatov Pomeron we study the deep inelastic limit. We find mixing between the four-gluon operator and a twist-four piece of the two-gluon operator. We calculate the diagonal elements of the matrix of the anomalous dimensions and the coefficient function of the singular part (near n=1) of the four-gluon operator. Several disagreements between our results and the Gribov-Levin-Ryskin evolution equation are found.

1 Introduction

The advent of the HERA machine opens the possibility of measuring the proton structure functions at very small values of Bjorken-x. The theoretical challenge of this new branch of QCD investigations lies in the fact that the small-x region lies at the interface between perturbative and nonperturbative QCD (Fig.1): starting from the quasi-free parton picture, and taking into account more and more QCD corrections one might hope to be able to penetrate into the nonperturbative region and eventually to approach the Regge limit of hadron-hadron scattering.

More concretely, several questions arise. The one concerns possible modifications of the linear Gribov-Lipatov-Altarelli-Parisi [1,2] evolution equation. The origin for the expected failure of the linear GLAP evolution scheme at small x is the singularity of the anomalous dimension at n=1 (n is the moment index). In the small-x region the structure functions become more and more sensitive to this singuarity, and this is why they eventually become too large. Now a closer inspection of the nonleading terms in the twist-expansion (which for not too small x are suppressed by powers of Q^2) shows that the corresponding anomalous dimensions are again singular at n=1. So for small x they also become large and eventually overcome the $1/Q^2$ suppression. This motivates a systematic calculation of the singular (at n=1) part of the first nonleading-twist term. The relevant operator is the four-gluon operator, since it contains, for a given order of α_s, the strongest singularity in n-1. Quanitites of interest are the anomalous dimension and the coefficient function. It is also not clear a proiri, whether this term has a partonic interpretation. On the longer run, one may think of carrying out such a calculation for all nonleading twist terms and try to sum them up.

Several years ago [3], it has been suggested that in certain parts of the small-x region, these equations need to be corrected by adding a certain nonlinear term. This term can be interpreted as describing new partonic interactions inside the proton, gluon-gluon recombination processes. Numerical estimates [4,5,6,7] which have been based upon this equation gave rise to the hope that - under favorable circumstances - these "screening" effects my be visible at HERA, either in the analysis of structure functions or, more likely, in what has been named "dedicated measurements". The derivation of this equation is complicated. Apart from certain assumptions - the validity of which only the experiment can decide - the basic claim is that this equation represents the sum of QCD-corrections to the GLAP- equation. On a certain line in the Q^2-x_B plane these corrections become as large as the GLAP equation itself, and from there on the validity of perturbation theory becomes questionable. Clearly it is necessary a better theoretical understanding of the derivation

of this equation: in what sense can this equation be "derived" from QCD?

Another topic that comes to mind in the context of small-x deep inelastic scattering is the gluon structure function and the so-called Balitzky-Fadin-Kuraev-Lipatov approximation [8,9,10,11,12] to the Pomeron (BFKL-Pomeron). One of the goals of HERA physics is a precise measurement of the gluon structure function at small x_B, in particular its x-dependence at fixed Q^2. It has been suggested several years ago that this behaviour should be described by - and hence would be a test for - the BFKL Pomeron which predicts a rather steep rise at small x. An even better test of the BFKL-Pomeron might be provided by the so-called "hot spot" jets [13,14,15,16,17,18]. In both cases there is no doubt that the BFKL-Pomeron is only the first approximation to a more complete (in particular: fully unitary) description, and in fact it may very well be that in the HERA domain where either the gluon structure function or the hot spot jets are measured, the BFKL-Pomeron may already partly be hidden behind its corrections. So there is an obvious need to derive these corrections and to calculate their size.

In fact, the answers to both questions are closely connected. The most dramatic defect of the BFKL Pomeron is the lack of unitarity: the leading high energy behaviour violates unitarity bounds, indicating that the restauration of unitarity must be the main guideline when discussing the corrections (there are also other corrections, such as, for example, higher order corrections to the BFKL kernel or the gluon trajectory function which will result in turning the fixed QCD-coupling into the running α_s). Generally speaking, unitarity corrections lead to t-channel states with an arbitrary number of (reggeized) gluons. The first correction beyond the BFKL Pomeron contains the four gluon states. It is expected (but not proven) that the high energy behavior of this contribution grows even stronger than the BFKL approximation. Returning to the higher-twist corrections to the GLAP evolution equations, we have argued that the first correction comes from the four gluon operator: it is therefore evident that both type of corrections should be closesly connected.

In fact, it seems very plausible to expect that, from the knowledge of the unitarity corrections to the BFKL Pomeron, one can derive the singular part of the four-gluon operator (whereas the inverse may not be true): the BFKL Pomeron and all its unitarity corrections collect, for each order α_s, the maximal number of powers of $\ln s/Q^2 = \ln \frac{1}{x_B}$. Translating this into angular momentum j, we are talking about the strongest singularity in $j-1=\omega$. Transverse momenta, on the other side, are not large; in fact the BFKL Pomeron has the attractive feature that it is finite also for very small transverse momenta. In the language of deep inelastic scattering, taking moments is the same

as projecting on Lorentz spin or angular momentum: singularities in $n-1$ are also the singularities in $j-1$. This suggests the following strategy (and the program of this paper): start from the four-gluon amplitudes as they appear in the first unitarity corrections to the BFKL Pomeron, and then take the limit of large Q^2/k_i^2 which is equivalent to the limit of short distances (k_i are the momenta of the four gluons). During this process one should keep in mind that in the BFKL Pomeron and its corrections the gluons are reggeized (i.e.composite), whereas the four-gluon operator in deep inelastic scattering deals with gluon fields. As a result, the four-gluon amplitude which form the start contain actually more than it is needed for the four gluon operator. We also remind the reader that the BFKL Pomeron - although it contains t-channel states with two reggeized gluons only - nevertheless contains terms which belong to the nonleading twist four. This is again a consequence of the reggeization, and in connection with the four gluon states it leads to mixing effects.

We can now define the outline of this paper. Starting point of our calculations are the unitarity corrections to the BFKL Pomeron. The whole program of how to find these correction has been outlined elswhere [] and will not be repeated here. We therefore begin with writing down the integral equations for these corrections (section 2) and discussing the solutions (section 3). As a very important consistency check, we show the infrared finiteness (section 4). Section 5 then contains the main part of this paper, namely the "deep inelastic limit". Results are the anomalous dimension of the four gluon operator, the mixing between the BFKL Pomeron and the four gluon states, and all the elements of the coefficient function. We also find evidence that the singular twist-four terms may allow a consistent partonic interpretation. We point out that there are severe discrepancies between our results and the GLR equation. Questions of any practical calculations will not be discussed in this paper but have to adressed in a future paper. Some results presented in this paper have been published in a letter [19].

2 The Integral Equations

We begin by writing down the explicit form of the integral equations for the partial waves D_2, D_3 and D_4. Throughout this paper we use the variable $\omega = j-1$, and the energy dependence (in the context of deep inelastic scattering: the dependence upon $\frac{1}{x}$) is obtained by the Mellin transform. The way these integral equations are derived is outlined in some detail in [20]. Here we only sketch the logic. As we have said in the introduction, our starting point are the first unitarity corrections to the BFKL Pomeron; they are defined to have t-channel states with four reggeized

gluons. Since the high energy behavior in the Regge limit is generally most easily described in terms of cross channel partial waves, we need to calculate the partial wave for the transition 2-particles $\to$ 4-(reggeized) gluons. The point of interest is angular momentum j=1 (or, in the language of moments, n=1). One starts from a six-point amplitude in the triple Regge limit (Fig.2a): $s_{12} = (p_1 + p_2)^2$, $s_{1'3'} = (p_{1'} + p_{3'})^2$, $s_{122'} = (p_1 + p_2 - p_{2'})^2 \to \infty$; $s_{122'}/s_{12}$, $s_{122'}/s_{1'3'} \ll 1$; $t_{12} = (p_1 - p_{1'})^2 = 0$; $t_{22'}$, $t_{33'} = O(1)$. The corresponding partial wave is given by a triple energy discontinuity (in s_{12}, $s_{122'}$, and $s_{1'3'}$) (Fig.2b) which is calculated from unitarity integrals. Its phase space is restricted to the multiperipheral region, and for the amplitudes $T_{2\to n}$. $T_{n\to m}$ we use the (real-valued) leading-lns approximations, as given for example in [20]. Signature in all three t-channels is introduced by adding (or subtracting) the proper s-u crossing terms. Finally, we move onto the nonsense pole at $j_{11'} = j_{22'} + j_{33'} - 1$ and take the two-reggeon cut in the $t_{22'}$ and $t_{33'}$ channel. Inserting these "residues" C_4 into the reggeon unitarity equations [22] for the partial wave of the $2 \to 2$ scattering amplitude (at the tip of the four-reggeon cut), and inserting the proper signature factors, one arrives at the partial waves (Fig.2c). For our purposes it will be necessary to allow all color quantum numbers and signatures in the $t_{22'}$ and $t_{33'}$ channels. In the $t_{11'}$ channel we restrict ourselves to color zero and even signature. Infrared problems do not arise, as we will discuss below. The results of this construction are represented in the form of coupled integral equations which we illustrate in Fig.3.

Before we present the details we mention that this construction is in agreement with the Abramovsky-Gribov-Kancheli [21] cutting rules: namely from these particle-reggeon amplitudes we construct, via the reggeon unitarity equations (Fig.2c), the $2 \to 2$ scattering amplitude (in our case, the process is the elastic scattering of a virtual photon on a proton). Inserting the correct signature factors, the whole contribution obtains a negative sign (the same as the usual minus sign of the two-Pomeron cut): consequently, the four-gluon contribution discussed in this paper has the opposite sign compared to the usual GLAP evolution equation. Next we could analyse the s-channel unitarity content. It is then possible to show that the same answer (including the negative sign) could have been obtained from the calculation of s-channel unitarity integrals directly (Fig.2d). For the present purposes, however, we shall not discuss this in detail. In this paper, we shall even not construct the scattering amplitude of the process $\gamma\star + proton \to \gamma\star + proton$, but concentrate on the "residue" function C_4 in the upper part of the reggeon unitarity equations (Fig.2a).

Let us now turn to the explicit form of the integral equations for the four gluon amplitude. When calculating the multiple energy discontinuities one first encounters the task of "squaring production

vertices". They lead to the kernels $K_{2\to 2}$, $K_{2\to 3}$ and $K_{2\to 4}$ which have the form (cf.eqs.(2.8), (2.18), (4.12) of I):

$$\frac{1}{g^2} K_{2\to 2}(k_1, k_2; k_1', k_2') = q^2 - \frac{k_1^2 k_2'^2 + k_2^2 k_1'^2}{(k_1 - k_1')^2}, \tag{2.1}$$

$$\frac{1}{g^3} K_{2\to 3}(k_1 k_2; k_1' k_2' k_3') = -q^2 + \frac{(k_1' + k_2')^2 k_2^2}{(k_2 - k_3')^2} + \frac{(k_2' + k_3')^2 k_1^2}{(k_1 - k_1')^2} - \frac{k_1^2 k_2^2 k_2'^2}{(k_1 - k_1')^2 (k_2 - k_3')^2}, \tag{2.2}$$

and

$$\frac{1}{g^4} K_{2\to 4}(k_1 k_2; k_1' k_2' k_3' k_4') = q^2 - \frac{(k_1' + k_2' + k_3')^2 k_2^2}{(k_2' - k_4')^2} - \frac{(k_2' + k_3' + k_4')^2 k_1^2}{(k_1 - k_1')^2} + \frac{k_1^2 k_2^2 (k_2' + k_3')^2}{(k_1 - k_1')^2 (k_2 - k_4')^2}. \tag{2.3}$$

Now we could already write down integral equations, but at this stage we are still dealing with SU(3) tensors with 6 color indices, and it is more convenient to first reduce the group structure and form signatured amplitudes: positive (negative) signature is defined as symmetry (antisymmetry) under the simultaneous exchange of momenta and group indices of two gluon lines. We chose the coupling scheme illustrated in Fig.2e. All necessary details of the group structure are collected in the appendix, and we proceed to write down the result.

For completeness we start with the equation for D_2 in the color singlet chanel (even signature), the so-called Balitzky-Fadin-Kuraev- Lipatov (BFKL) equation:

$$\omega D_2(k_1, k_2; \omega) = D_{(2;0)} + D_2 \otimes (c_i K_{2\to 2}(k_1, k_2) + \alpha(k_1) + \alpha(k_2) - 2). \tag{2.4}$$

with $c_i = -3, -\frac{3}{2}, -\frac{3}{2}, 0, 1$ for $i = 1, 8_A, 8_S, 10 + \overline{10}, 27$, resp. We shall need only the color singlet c_1=-3. We have used the abbreviation: $\otimes = \int \frac{d^2k}{(2\pi)^3} \cdot$ *gluon propagators*. The trajectory function is:

$$\begin{aligned} \alpha(t) &= 1 + \frac{3}{2} t \beta_2(t) \\ \beta_2(t) &= g^2 \int \frac{d^2k}{(2\pi)^3} \frac{1}{k^2 (k-q)^2} \\ t &= -k^2. \end{aligned} \tag{2.5}$$

The inhomogeneous term $D_{(2;0)}$ stands for the coupling of two gluons to two virtual photons: to lowest order in g^2, this is just a closed fermion loop with the gluons attached in all possible ways. The analytic form for this coupling can be found in [23] and will not be repeated here. Further

$$\omega \begin{pmatrix} D_4^{(1;--)}(\omega;k_1,k_2,k_3,k_4) \\ D_4^{(8_A;--)}(\omega;k_1,k_2,k_3,k_4) \\ D_4^{(8_S;--)}(\omega;k_1,k_2,k_3,k_4) \\ D_4^{(10+\overline{10};--)}(\omega;k_1,k_2,k_3,k_4) \\ D_4^{(27;--)}(\omega;k_1,k_2,k_3,k_4) \end{pmatrix} = \begin{pmatrix} D_{(4;0)}^{(1;--)}(k_1,k_2,k_3,k_4) \\ D_{(4;0)}^{(8_A;--)}(k_1,k_2,k_3,k_4) \\ D_{(4;0)}^{(8_S;--)}(k_1,k_2,k_3,k_4) \\ D_{(4;0)}^{(10+\overline{10};--)}(k_1,k_2,k_3,k_4) \\ D_{(4;0)}^{(27;--)}(k_1,k_2,k_3,k_4) \end{pmatrix} + D_2 \otimes \begin{pmatrix} \frac{9}{\sqrt{8}} K_{2\to 4}([k_1,k_2][k_3,k_4]) \\ \frac{\sqrt{6}}{4} K_{2\to 4}(\{k_1,k_2\}\{k_3,k_4\}) \\ \frac{9}{4} K_{2\to 4}([k_1,k_2][k_3,k_4]) \\ 0 \\ \frac{3\sqrt{3}}{\sqrt{8}} K_{2\to 4}([k_1,k_2][k_3,k_4]) \end{pmatrix}$$

$$- \begin{pmatrix} 3\sqrt{\frac{3}{8}}[D_3^{(-)}(k_a\{k_bk_4\}) \otimes K_{2\to 3}([k_1k_2]k_3) - D_3^{(-)}(k_a\{k_bk_3\}) \otimes K_{2\to 3}([k_1k_2]k_4) + D_3^{(-)}(\{k_1k_a\}k_b) \otimes K_{2\to 3}(k_2[k_3k_4]) - D_3^{(-)}(\{k_2k_a\}k_b) \otimes K_{2\to 3}(k_1[k_3k_4])] \\ \frac{3\sqrt{3}}{4}[D_3^{(-)}(k_a\{k_bk_4\}) \otimes K_{2\to 3}(\{k_1k_2\}k_3) + D_3^{(-)}(k_a\{k_bk_3\}) \otimes K_{2\to 3}(\{k_1k_2\}k_4) + D_3^{(-)}(\{k_1k_a\}k_b) \otimes K_{2\to 3}(k_2\{k_3k_4\}) + D_3^{(-)}(\{k_2k_a\}k_b) \otimes K_{2\to 3}(k_1\{k_3k_4\})] \\ \frac{3\sqrt{3}}{4}[D_3^{(-)}(k_a\{k_bk_4\}) \otimes K_{2\to 3}([k_1k_2]k_3) - D_3^{(-)}(k_a\{k_bk_3\}) \otimes K_{2\to 3}([k_1k_2]k_4) + D_3^{(-)}(\{k_1k_a\}k_b) \otimes K_{2\to 3}(k_2[k_3k_4]) - D_3^{(-)}(\{k_2k_a\}k_b) \otimes K_{2\to 3}(k_1[k_3k_4])] \\ 0 \\ \frac{3}{\sqrt{8}}[D_3^{(-)}(k_a\{k_bk_4\}) \otimes K_{2\to 3}([k_1k_2]k_3) - D_3^{(-)}(k_a\{k_bk_3\}) \otimes K_{2\to 3}([k_1k_2]k_4) + D_3^{(-)}(\{k_1k_a\}k_b) \otimes K_{2\to 3}(k_2[k_3k_4]) - D_3^{(-)}(\{k_2k_a\}k_b) \otimes K_{2\to 3}(k_1[k_3k_4])] \end{pmatrix}$$

$$+ \begin{pmatrix} D_4^{(1;--)} \\ D_4^{(8_A;--)} \\ D_4^{(8_S;--)} \\ D_4^{(10+\overline{10};--)} \\ D_4^{(27;--)} \end{pmatrix}^T \otimes \begin{pmatrix} -3Q_{(12)(34)}+\Sigma & \frac{3}{\sqrt{8}}(-Q_{(14)(23)}+Q_{(13)(24)}) & & & \\ \frac{3}{\sqrt{8}}(-Q_{(14)(23)}+Q_{(13)(24)}) & \begin{matrix} -\frac{3}{2}Q_{(12)(34)}+\Sigma \\ -\frac{3}{4}(Q_{(14)(23)}+Q_{(13)(24)}) \end{matrix} & \frac{3}{4}(-Q_{(14)(23)}+Q_{(13)(24)}) & & \sqrt{\frac{3}{8}}(-Q_{(14)(23)}+Q_{(13)(24)}) \\ & \frac{3}{4}(-Q_{(14)(23)}+Q_{(13)(24)}) & \begin{matrix} -\frac{3}{2}Q_{(12)(34)}+\Sigma \\ -\frac{3}{4}(Q_{(14)(23)}+Q_{(13)(24)}) \end{matrix} & \frac{3}{\sqrt{10}}(-Q_{(14)(23)}+Q_{(13)(24)}) & \\ & & \frac{3}{\sqrt{10}}(-Q_{(14)(23)}+Q_{(13)(24)}) & \begin{matrix} \Sigma \\ -\frac{3}{2}(Q_{(13)(24)}+Q_{(14)(23)}) \end{matrix} & \sqrt{\frac{3}{5}}(-Q_{(14)(23)}+Q_{(13)(24)}) \\ & \sqrt{\frac{3}{8}}(-Q_{(14)(23)}+Q_{(13)(24)}) & & \sqrt{\frac{3}{5}}(-Q_{(14)(23)}+Q_{(13)(24)}) & \begin{matrix} Q_{(12)(34)}+\Sigma \\ -2(Q_{(14)(23)}+Q_{(13)(24)}) \end{matrix} \end{pmatrix} \tag{1}$$

(2.10)

below we shall make use of the following expansion near $k_1^2 = k_2^2 = 0$ (for a quark with charge e_q):

$$D_{(2;0)}(k_1,-k_1) = \frac{\alpha_s e_q^2}{2\pi}\left(-\frac{2}{3}r_1\ln r_1 + \frac{7}{9}r_1 + \frac{1}{5}r_1^2 + O(r_1^3\ln r_1)\right) \tag{2.6}$$

with $r_1 = k_1^2/Q^2$. This is an expansion in inverse powers of Q^2: correspondingly, the first two term will be referred to as "twist-two", the third one as twist-four, etc. (our normalization is such that, in order to obtain a deep-inelastic structure function, our D-functions are multiplied by Q^2; this is why we associate the leading term with "twist-two"). Note that the logarithmic contribution of the twist-four term is absent.

Next the three-reggeon case:

$$\begin{aligned} &\omega D_3^{(-)}(k_1,k_2,k_3;\omega) = D_{(3;0)}^{(-)}(k_1,k_2,k_3) + \tfrac{3\sqrt{3}}{2} D_2 \otimes K_{2\to 3}(k_1\{k_2k_3\}) \\ &+ D_3^{(-)} \otimes [-\tfrac{3}{2}K_{2\to 2}(k_2k_3) + \alpha(k_1) + \alpha(k_2) + \alpha(k_3) - 3 - \tfrac{3}{2}K_{2\to 2}(k_1k_2) - \tfrac{3}{2}K_{2\to 2}(k_1k_3)] \\ &\omega D_3^{(+)}(k_1,k_2,k_3;\omega) = D_{(3;0)}^{(+)}(k_1,k_2,k_3) + \tfrac{3\sqrt{3}}{2} D_2 \otimes K_{2\to 3}(k_1\{k_2k_3\}) \\ &+ D_3^{(+)} \otimes [-\tfrac{3}{2}K_{2\to 2}(k_2k_3) + \alpha(k_1) + \alpha(k_2) + \alpha(k_3) - 3 - \tfrac{3}{2}K_{2\to 2}(k_1k_2) - \tfrac{3}{2}K_{2\to 2}(k_1k_3)]. \end{aligned} \tag{2.7}$$

The superscript of D_3 refers to the signature of the (23) subsystem. For the total system we restrict ourselves to the color singlet and even signature configuration; the (23) system then is always in the 8_A representation. The inhomogeneous terms again stand for a closed fermion loop with the three gluons being attached in all possible ways. The analytic form follows from [23]:

$$D_{(3;0)}^{(-)}(k_1,k_2,k_3) = g\frac{\sqrt{3}}{2} D_{(2;0)}(k_1,k_2+k_3;\omega) \tag{2.8}$$

and

$$D_{(3;0)}^{(+)}(k_1,k_2,k_3) = g\frac{\sqrt{3}}{2}[D_{(2;0)}(k_1+k_2,k_3;\omega) - D_{(2;0)}(k_1+k_3,k_2;\omega)]. \tag{2.9}$$

Finally the case of the four-reggeon amplitude. The outgoing gluons are grouped into two pairs, (12) and (34); since the total color charge must be zero, both subsystems have identical color quantum numbers. For the signature assignment we have the possibilities (-,-), (+,+), and (+,-), which will be labeled by corresponding superscripts. The sets of integral equations (which preserve signature) are given on the three following pages:

$$\omega \begin{pmatrix} D_4^{(1;++)}(\omega;k_1,k_2,k_3,k_4) \\ D_4^{(8_A;++)}(\omega;k_1,k_2,k_3,k_4) \\ D_4^{(8_S;++)}(\omega;k_1,k_2,k_3,k_4) \\ D_4^{(10+\bar{10};++)}(\omega;k_1,k_2,k_3,k_4) \\ D_4^{(27;++)}(\omega;k_1,k_2,k_3,k_4) \end{pmatrix} = \begin{pmatrix} D_{(4;0)}^{(1;++)}(k_1,k_2,k_3,k_4) \\ D_{(4;0)}^{(8_A;++)}(k_1,k_2,k_3,k_4) \\ D_{(4;0)}^{(8_S;++)}(k_1,k_2,k_3,k_4) \\ D_{(4;0)}^{(10+\bar{10};++)}(k_1,k_2,k_3,k_4) \\ D_{(4;0)}^{(27;++)}(k_1,k_2,k_3,k_4) \end{pmatrix} + D_2 \otimes \begin{pmatrix} \frac{9}{\sqrt{8}} K_{2\to 4}(\{k_1,k_2\}\{k_3,k_4\}) \\ \frac{9}{4} K_{2\to 4}([k_1,k_2][k_3,k_4]) \\ \frac{9}{4} K_{2\to 4}(\{k_1,k_2\}\{k_3,k_4\}) \\ 0 \\ \frac{3\sqrt{3}}{\sqrt{8}} K_{2\to 4}(\{k_1,k_2\}\{k_3,k_4\}) \end{pmatrix}$$

$$- \begin{pmatrix} 3\sqrt{\frac{3}{8}}[D_3^{(+)}(k_a[k_bk_4]) \otimes K_{2\to 3}(\{k_1k_2\}k_3) + D_3^{(+)}(k_a[k_bk_3]) \otimes K_{2\to 3}(\{k_1k_2\}k_4) + D_3^{(+)}([k_1k_a]k_b) \otimes K_{2\to 3}(k_2\{k_3k_4\}) + D_3^{(+)}([k_2k_a]k_b) \otimes K_{2\to 3}(k_1\{k_3k_4\})] \\ \frac{3\sqrt{3}}{4}[D_3^{(+)}(k_a[k_bk_4]) \otimes K_{2\to 3}([k_1k_2]k_3) - D_3^{(+)}(k_a[k_bk_3]) \otimes K_{2\to 3}([k_1k_2]k_4) + D_3^{(+)}([k_1k_a]k_b) \otimes K_{2\to 3}(k_2[k_3k_4]) - D_3^{(+)}([k_2k_a]k_b) \otimes K_{2\to 3}(k_1[k_3k_4])] \\ \frac{3\sqrt{3}}{4}[D_3^{(+)}(k_a[k_bk_4]) \otimes K_{2\to 3}(\{k_1k_2\}k_3) + D_3^{(+)}(k_a[k_bk_3]) \otimes K_{2\to 3}(\{k_1k_2\}k_4) + D_3^{(+)}([k_1k_a]k_b) \otimes K_{2\to 3}(k_2\{k_3k_4\}) + D_3^{(+)}([k_2k_a]k_b) \otimes K_{2\to 3}(k_1\{k_3k_4\})] \\ 0 \\ \frac{3}{\sqrt{8}}[D_3^{(+)}(k_a[k_bk_4]) \otimes K_{2\to 3}(\{k_1k_2\}k_3) + D_3^{(+)}(k_a[k_bk_3]) \otimes K_{2\to 3}(\{k_1k_2\}k_4) + D_3^{(+)}([k_1k_a]k_b) \otimes K_{2\to 3}(k_2\{k_3k_4\}) + D_3^{(+)}([k_2k_a]k_b) \otimes K_{2\to 3}(k_1\{k_3k_4\})] \end{pmatrix}$$

$$+ \begin{pmatrix} D_4^{(1;++)} \\ D_4^{(8_A;++)} \\ D_4^{(8_S;++)} \\ D_4^{(10+\bar{10};++)} \\ D_4^{(27;++)} \end{pmatrix}^T \otimes \begin{pmatrix} -3Q_{(12)(34)}+\Sigma & \frac{3}{\sqrt{8}}(-Q_{(14)(23)}+Q_{(13)(24)}) & & & \\ \frac{3}{\sqrt{8}}(-Q_{(14)(23)}+Q_{(13)(24)}) & -\frac{3}{2}Q_{(12)(34)}+\Sigma & \frac{3}{4}(-Q_{(14)(23)}+Q_{(13)(24)}) & & \sqrt{\frac{3}{8}}(-Q_{(14)(23)}+Q_{(13)(24)}) \\ & -\frac{3}{4}(Q_{(14)(23)}+Q_{(13)(24)}) & & & \\ & \frac{3}{4}(-Q_{(14)(23)}+Q_{(13)(24)}) & -\frac{3}{2}Q_{(12)(34)}+\Sigma & \frac{3}{\sqrt{10}}(-Q_{(14)(23)}+Q_{(13)(24)}) & \\ & & -\frac{3}{4}(Q_{(14)(23)}+Q_{(13)(24)}) & & \\ & & \frac{3}{\sqrt{10}}(-Q_{(14)(23)}+Q_{(13)(24)}) & \Sigma & \sqrt{\frac{3}{5}}(-Q_{(14)(23)}+Q_{(13)(24)}) \\ & & & -\frac{3}{2}(Q_{(13)(24)}+Q_{(14)(23)}) & \\ & \sqrt{\frac{3}{8}}(-Q_{(14)(23)}+Q_{(13)(24)}) & & \sqrt{\frac{3}{5}}(-Q_{(14)(23)}+Q_{(13)(24)}) & Q_{(12)(34)}+\Sigma \\ & & & & -2(Q_{(14)(23)}+Q_{(13)(24)}) \end{pmatrix}$$

(2.11) (2)

$$\omega \begin{pmatrix} D_4^{(1;+-)}(\omega;k_1,k_2,k_3,k_4) \\ D_4^{(8_A;+-)}(\omega;k_1,k_2,k_3,k_4) \\ D_4^{(8_S;+-)}(\omega;k_1,k_2,k_3,k_4) \\ D_4^{(10+\bar{10};+-)}(\omega;k_1,k_2,k_3,k_4) \\ D_4^{(27;+-)}(\omega;k_1,k_2,k_3,k_4) \end{pmatrix} = \begin{pmatrix} D_4^{(1;+-)}(\omega;k_1,k_2,k_3,k_4) \\ D_4^{(8_A;+-)}(\omega;k_1,k_2,k_3,k_4) \\ D_4^{(8_S;+-)}(\omega;k_1,k_2,k_3,k_4) \\ D_4^{(10+\bar{10};+-)}(\omega;k_1,k_2,k_3,k_4) \\ D_4^{(27;+-)}(\omega;k_1,k_2,k_3,k_4) \end{pmatrix} + D_2^{(1;+)} \otimes \begin{pmatrix} \frac{9}{\sqrt{8}} K_{2\to 4}(\{k_1,k_2\}[k_3,k_4]) \\ \frac{9}{4} K_{2\to 4}([k_1,k_2]\{k_3,k_4\}) \\ \frac{9}{4} K_{2\to 4}(\{k_1,k_2\}[k_3,k_4]) \\ 0 \\ \frac{3\sqrt{3}}{\sqrt{8}} K_{2\to 4}(\{k_1,k_2\}[k_3,k_4]) \end{pmatrix}$$

$$- \begin{pmatrix} 3\sqrt{\frac{3}{8}}[D_3^{(-)}(k_a\{k_bk_4\}) \otimes K_{2\to 3}(\{k_1k_2\}k_3) - D_3^{(-)}(k_a\{k_bk_3\}) \otimes K_{2\to 3}(\{k_1k_2\}k_4) + D_3^{(+)}([k_1k_a]k_b) \otimes K_{2\to 3}(k_2[k_3k_4]) + D_3^{(+)}([k_2k_a]k_b) \otimes K_{2\to 3}(k_1[k_3k_4])] \\ \frac{3\sqrt{3}}{4}[D_3^{(-)}(k_a\{k_bk_4\}) \otimes K_{2\to 3}([k_1k_2]k_3) + D_3^{(-)}(k_a\{k_bk_3\}) \otimes K_{2\to 3}([k_1k_2]k_4) + D_3^{(+)}([k_1k_a]k_b) \otimes K_{2\to 3}(k_2\{k_3k_4\}) - D_3^{(+)}([k_2k_a]k_b) \otimes K_{2\to 3}(k_1\{k_3k_4\})] \\ \frac{3\sqrt{3}}{4}[D_3^{(-)}(k_a\{k_bk_4\}) \otimes K_{2\to 3}(\{k_1k_2\}k_3) - D_3^{(-)}(k_a\{k_bk_3\}) \otimes K_{2\to 3}(\{k_1k_2\}k_4) + D_3^{(+)}([k_1k_a]k_b) \otimes K_{2\to 3}(k_2[k_3k_4]) + D_3^{(+)}([k_2k_a]k_b) \otimes K_{2\to 3}(k_1[k_3k_4])] \\ 0 \\ \frac{3}{\sqrt{8}}[D_3^{(-)}(k_a\{k_bk_4\}) \otimes K_{2\to 3}(\{k_1k_2\}k_3) - D_3^{(-)}(k_a\{k_bk_3\}) \otimes K_{2\to 3}(\{k_1k_2\}k_4) + D_3^{(+)}([k_1k_a]k_b) \otimes K_{2\to 3}(k_2[k_3k_4]) + D_3^{(+)}([k_2k_a]k_b) \otimes K_{2\to 3}(k_1[k_3k_4])] \end{pmatrix}$$

$$+ \begin{pmatrix} D_4^{(1;+-)} \\ D_4^{(8_A;+-)} \\ D_4^{(8_S;+-)} \\ D_4^{(10+\bar{10};+-)} \\ D_4^{(27;+-)} \end{pmatrix}^T \otimes \begin{pmatrix} -3Q_{(12)(34)}+\Sigma & \frac{3}{\sqrt{8}}(-Q_{(14)(23)}+Q_{(13)(24)}) & & & \\ \frac{3}{\sqrt{8}}(-Q_{(14)(23)}+Q_{(13)(24)}) & -\frac{3}{2}Q_{(12)(34)}+\Sigma & \frac{3}{4}(-Q_{(14)(23)}+Q_{(13)(24)}) & & \sqrt{\frac{3}{8}}(-Q_{(14)(23)}+Q_{(13)(24)}) \\ & -\frac{3}{4}(Q_{(14)(23)}+Q_{(13)(24)}) & & & \\ & \frac{3}{4}(-Q_{(14)(23)}+Q_{(13)(24)}) & -\frac{3}{2}Q_{(12)(34)}+\Sigma & \frac{3}{\sqrt{10}}(-Q_{(14)(23)}+Q_{(13)(24)}) & \\ & & -\frac{3}{4}(Q_{(14)(23)}+Q_{(13)(24)}) & & \\ & & \frac{3}{\sqrt{10}}(-Q_{(14)(23)}+Q_{(13)(24)}) & \Sigma & \sqrt{\frac{3}{5}}(-Q_{(14)(23)}+Q_{(13)(24)}) \\ & & & -\frac{3}{2}(Q_{(13)(24)}+Q_{(14)(23)}) & \\ & \sqrt{\frac{3}{8}}(-Q_{(14)(23)}+Q_{(13)(24)}) & & \sqrt{\frac{3}{5}}(-Q_{(14)(23)}+Q_{(13)(24)}) & Q_{(12)(34)}+\Sigma \\ & & & & -2(Q_{(14)(23)}+Q_{(13)(24)}) \end{pmatrix}$$

(2.12) (3)

The structure of these equations is illustrated in Fig.3. We have used the abbrevations:

$$\begin{aligned}\Sigma &= \sum_1^4(\alpha(k_i)-1),\\ Q_{(12)(34)} &= K_{2\to 2}(k_1,k_2)+K_{2\to 2}(k_3,k_4).\end{aligned} \tag{2.13}$$

The superscripts of D_4 refer to color and signature of the (12) and the (34) subsystems; the full system is always in the color singlet state and carries even signature. The inhomogeneous terms again denote a closed fermion loop with the four gluons being attached in all possible ways. The analytic form which will be derived elsewhere [23] turns out to be very simple. $D_{(4;0)}$ can be expressed as a sum of $D_{(2;0)}$ functions (cf.eq.(2.6)):

$$\begin{aligned}D^{(1;++)}_{(4;0)}(k_1,k_2,k_3,k_4) &= \\ &-g^2\frac{\sqrt{2}}{3}\Big(D_{(2;0)}(k_1,k_2+k_3+k_4;\omega)+D_{(2;0)}(k_i+k_2+k_3,k_4;\omega)\\ &+D_{(2;0)}(k_1+k_2+k_4,k_3;\omega)+D_{(2;0)}(k_2,k_1+k_3+k_4;\omega)\\ &-D_{(2;0)}(k_1+k_2,k_3+k_4;\omega)-D_{(2;0)}(k_1+k_3,k_2+k_4;\omega)\\ &-D_{(2;0)}(k_1+k_4,k_2+k_3;\omega)\Big)\end{aligned} \tag{2.14}$$

$$\begin{aligned}D^{(8_A;++)}_{(4;0)}(k_1,k_2,k_3,k_4;\omega) &= \\ &-g^2\frac{3}{4}\Big(D_{(2;0)}(k_1+k_3,k_2+k_4;\omega)-D_{(2;0)}(k_1+k_4,k_2+k_3;\omega)\Big)\end{aligned} \tag{2.15}$$

$$D^{(8_A;--)}_{(4;0)}(k_1,k_2,k_3,k_4;\omega) = -g^2\frac{3}{4}D_{(2;0)}(k_1+k_2,k_3+k_4;\omega) \tag{2.16}$$

$$\begin{aligned}D^{(8_A;+-)}_{(4;0)}(k_1,k_2,k_3,k_4;\omega) &= \\ &-g^2\frac{3}{4}\Big(D_{(2;0)}(k_1,k_2+k_3+k_4;\omega)-D_{(2;0)}(k_2,k_1+k_3+k_4;\omega)\Big)\end{aligned} \tag{2.17}$$

$$\begin{aligned}D^{(8_S;++)}_{(4;0)}(k_1,k_2,k_3,k_4;\omega) &= \\ &-g^2\frac{5}{12}\left(D_2(k_1,k_2+k_3+k_4;\omega)+D_2(k_1+k_2+k_3,k_4;\omega)\right.\\ &+D_2(k_1+k_2+k_4,k_3;\omega)+D_2(k_2,k_1+k_3+k_4;\omega)\\ &-D_2(k_1+k_2,k_3+k_4;\omega)-D_2(k_1+k_3,k_2+k_4;\omega)\\ &\left.-D_2(k_1+k_4,k_2+k_3;\omega)\right).\end{aligned} \tag{2.18}$$

For all other color or signature configurations the fermion loop gives zero contribution. Among the properties that follow from these identities we only mention that for the color singlet and the symmetric octet the expressions vanish if any of the four momonta k_i goes to zero. For the antisymmetric color octet this is not the case. Instead, the D_4 amplitude becomes equal to the coresponding D_3 amplitudes.

3 Solutions

As it has been discussed in some detail in I, it is possible to find "solutions" to these equations. They are most easily discussed in the language of reggeon amplitudes, more precisely in terms of signature conservation. Let us start with the three-reggeon amplitudes. According to these rules, the even-signature t-channel cannot contain any odd-signature two-reggeon subsystem. Consequently, the D_3^- amplitudes must either vanish or two lines collapse into one single line (reggeization). In fact, one finds:

$$D_3^{(-)}(k_1,k_2,k_3;\omega) = g\cdot\frac{\sqrt{3}}{2}D_2(k_1,k_2+k_3;\omega). \tag{3.1}$$

For the other amplitude one finds:

$$D_3^{(+)}(k_1,k_2,k_3;\omega) = g\cdot\frac{\sqrt{3}}{2}[D_2(k_1+k_2,k_3;\omega)-D_2(k_1+k_3,k_2;\omega)]. \tag{3.2}$$

As a result, there is no three-reggeon state in the t-channel.

For the four-reggeon amplitude the situation is quite analogous: signature conservation requires that there is no odd number of reggeons. In fact, the only place where a three-reggeon state could appear is inside the inhomogeneous term with D_3, but because of (3.1) and (3.2) the three-reggeon state is in fact absent. Next we have to look into the reggeization. The easiest case is the state where the (12) and (34) subsystems have the quantum number of the gluon, i.e. they have odd signature and they are in the $(8)_A$ representation. One finds:

$$D_4^{(8_A;--)}(k_1,k_2,k_3,k_4;\omega) = -g^2\cdot\frac{3}{4}D_2(k_1+k_2,k_3+k_4;\omega). \tag{3.3}$$

In the symmetric color representations $(1),(8)_S$, and (27), odd signature would correspond to "wrong statistics". Also, a two-reggeon state consisting of two odd-signature reggeons cannot have odd signature. In fact, these amplitudes are identically zero:

$$D_4^{(1;--)} = D_4^{(8_S;--)} = D_4^{(10+\overline{10};--)} = D_4^{(27;--)} = 0. \tag{3.4}$$

For the case where both subsystems have even signature, the rules of signature conservation rules do not impose any restriction on the four- reggeon states, so we do not expect any particular simplification. The only feature we wish to emphasize is that, because of (3.1) and (3.2), the three-reggeon state cancels and the D_4-amplitude can be written as the sum over diagrams with two ort four (reggeizing) gluons. The transition from the two-gluon to the four-gluon state defines a "transition vertex".

For our subsequent derivation of anomalous dimensions it will be convenient to rewrite the integral equations: all our amplitudes D_4 still contain pieces with two-reggeon cuts only, and they do not contribute to the new four-gluon anomalous dimension. As we shall discuss below, for the antisymmetric octet channel it is necessary to subtfact these pieces from the rest of the amplitude; for the other color numbers it is convenient but not necessary. The existence of the two-reggeon cut pieces can be seen as follows. Instead of choosing, for both color and signature, the coupling scheme (12) and (34), we could as well have decided to couple reggeon 1 to reggeon 4, reggeon 2 to 3 (or any other scheme). We do not write down the corresponding equation, but merely note that in the $(8)_A$ color representation and odd signature for the (23) and (14) subsystems we find the solution

$$-g^2\frac{3}{4}[-D_2(k_1+k_4,k_2+k_3;\omega)+D_2(k_1+k_2+k_3,k_4;\omega)+D_2(k_1,k_2+k_2+k_4;\omega)], \qquad (3.5)$$

whereas the same color assignment with mixed signature gives zero. In other words, reggeization also holds in the other coupling schemes. Transforming in color space back to the previous (12), (34) coupling scheme one finds that there also the even signature channels $(1),(8)_A$ and $(8)_S$ must contain pieces with only two-reggeon states. They are:

$$\begin{aligned} D^{(1;++)}_{(4;2-cut)}(k_1,k_2,k_3,k_4;\omega) \;=\; & \\ & -g^2\frac{\sqrt{2}}{3}[D_2(k_1,k_2+k_3+k_4;\omega)+D_2(k_1+k_2+k_3,k_4;\omega) \\ & +D_2(k_1+k_2+k_4,k_3;\omega)+D_2(k_2,k_1+k_3+k_4;\omega) \\ & -D_2(k_1+k_2,k_3+k_4;\omega)-D_2(k_1+k_3,k_2+k_4;\omega) \\ & -D_2(k_1+k_4,k_2+k_3;\omega)] \end{aligned} \qquad (3.6)$$

$$D^{(8_A;++)}_{(4;2-cut)}(k_1,k_2,k_3,k_4;\omega)=-g^2\frac{3}{4}[D_2(k_1+k_3,k_2+k_4)-D_2(k_1+k_4,k_2+k_3)] \qquad (3.7)$$

$$D^{(8_S;++)}_{(4;2-cut)}(k_1,k_2,k_3,k_4;\omega) \;=$$

$$\begin{aligned} & -g^2\frac{5}{12}[D_2(k_1,k_2+k_3+k_4;\omega)+D_2(k_1+k_2+k_3,k_4;\omega) \\ & +D_2(k_1+k_2+k_4,k_3;\omega)+D_2(k_2,k_1+k_3+k_4;\omega) \\ & -D_2(k_1+k_2,k_3+k_4;\omega)-D_2(k_1+k_3,k_2+k_4;\omega) \\ & -D_2(k_1+k_4,k_2+k_3;\omega)]. \end{aligned} \qquad (3.8)$$

(In fact, this is the generalization of the form of the inhomogeneous terms $D_{(4;0)}$ in eqs.(2.14-18): in these lowest order expressions, there is nothing but the beginning of the formation of the two-reggeon cut. It is only in the next order of g^2 that the four-reggeon cut starts to be built up.)

Using now this information we write

$$D_4=D_{(4;2-cut)}+D_{(4;R)}. \qquad (3.9)$$

Inserting this ansatz into the integral equations for the D_4 and subtracting $D_{(4;2-cut)}$, the resulting equations for $D_{(4;R)}$ are of the form:

$$\begin{aligned} D_{(4;R)}=D_2\otimes K_{2\to4}+D_3\otimes\sum K_{2\to3}+D_{4;0}-D_{(4;2-cut)}+D_{(4;2-cut)}\otimes\sum(K_{2\to2}+\alpha-1) \\ +D_{(4;R)}\otimes\sum(K_{2\to2}+\alpha-1). \end{aligned} \qquad (3.10)$$

Compared to the original form (2.10)-(2.12), the inhomogeneous terms have changed, but not the kernels of the four-reggeon state. Further simplification is obtained if we make use of the integral equations for the various $D_2's$ inside the $D_{(4;2-cut)}$: from (3.7),(2.4), and (2.14) - (2.18) we obtain:

$$\begin{aligned} D_{(4;R)}=D_2\otimes K_{2\to4}+D_3\otimes\sum K_{2\to3}-\sum D_2\otimes K_{2\to2}+D_{(4;2-cut)}\otimes\sum(K_{2\to2}+\alpha-1) \\ +D_{(4;R)}\otimes\sum(K_{2\to2}+\alpha-1). \end{aligned} \qquad (3.11)$$

Again the inhomogenous terms have changed. Using for the second term eqs.(3.1) and (3.2), all inhomogenous terms are expressed in terms of D_2, and what they are multiplied with defines an "effective vertex for the transition two-gluons $\to$ four-gluons". It is this form of the integral equations that we shall use when studying the deep-inelastic limit (Fig.4). Note that the transition vertex defined through (3.11) is different from the one which follows from the original equations (2.10) - (2.12). In fact, as we shall discuss below, there is no unique definition of such a vertex.

Finally the case of mixed signature. We find:

$$D_4^{(1;+-)}=D_4^{(8_S;+-)}=D_4^{(10+\overline{10};+-)}=D_4^{(27;+-)}=0, \qquad (3.12)$$

and

$$D_4^{(8_A;+-)}(k_1,k_2,k_3,k_4;\omega)=g^2\frac{3}{4}[D_2(k_1,k_2+k_3+k_4;\omega)-D_2(k_2,k_1+k_3+k_4;\omega)]. \qquad (3.13)$$

4 Infrared Behavior

The next feature of the reggeon amplitudes that we wish to illustrate is the absence of infrared divergencies. This will be shown first for nonvanishing external momenta. We then show for D_2 and D_4 that they vanish if any of its external momenta goes to zero. The difficult task of computing the logarithms which accompany these zeroes and produce the anomalous dimensions will be postponed to the following section.

We begin with a brief repeat of the cancellation of infrared divergencies in D_2. To be general we consider the nonforward direction with $(k_1+k_2)^2 = q^2 \neq 0$, and in the integral equation we allow for any inhomogeneous term with the property

$$D_{(2;0)}(k_1,k_2;\omega) = O(|k_1|\cdot|k_2|). \tag{4.1}$$

We transform eq.(2.4) into a recursion relation: to lowest order, we have the inhomogeneous term with (4.1). The recursion relation reads:

$$D_{2,n+1} = D_{2,n} \otimes [-3K_{2\to 2}(k_1,k_2) + \alpha(k_1) + \alpha(k_2) - 2], \tag{4.2}$$

or, in more detail:

$$\begin{aligned} D^{(1;+)}_{2,n+1}(k,k-q;\omega) &= g^2 \int \frac{d^2k'}{(2\pi)^3} \\ &\left(D^{(1;+)}_{2,n}(k',q-k';\omega)\frac{1}{k'^2(q-k')^2}[-3q^2 + 3\frac{k'^2(q-k)^2}{(k-k')^2} + 3\frac{k^2(q-k')^2}{(k-k')^2}] \right. \\ &\left. -3D^{(1;+)}_{2,n}(k,q-k;\omega)[\frac{k^2}{(k-k')^2((k-k')^2+k'^2)} + \frac{(q-k)^2}{(k-k')^2((k-k')^2+(q-k')^2)}] \right). \end{aligned} \tag{4.3}$$

Let us label these five terms by a,b,c,d,e, resp., and let us assume that all external momenta k^2, $(q-k)^2$, and q^2 are different from zero. It is then easily seen that all infrared singularities cancel: the pole at $k=k'$ is absent if term "b" is combined with term "d", term "c" with "e". The trajectory function of the gluon thus serves as a regulator of this infrared singularity. The singularity near $k'=0$ cancels in the combination "a"+"c", similarly the pole near $k'=q$ in the combination "a"+"b". So the whole integral (4.3) is free from infrared divergencies (note that so far we have not made use of (4.1)). Next we take k to zero (with q^2 nonzero): if we first ignore the singularity near $k=k'=0$, terms "a" and "b" are seen to cancel against each other, whereas all the other terms vanish by themselves. A careful study of the region near $k'=0$ shows that we have to combine "a", "b", and "d", in order to obtain a finite expression of the form $O(|k|)$. As

a result, property (4.1) is preserved, and no logarithm is obtained. The same holds for the case $q-k=0$. For the study of D_4 it will be useful to keep in mind that it is the special combination of the kernel with the trajectory functions

$$-3K_{2\to 2}(k_1,k_2) + \alpha(k_1) + \alpha(k_2) - 2. \tag{4.4}$$

which we have shown to be infrared finite and to preserve the property (4.1). We shall refer to it as the (regularized) BFKL kernel. What remains to be investigated is the behaviour for small external virtualities in the forward direction, i.e. the limit $k_1^2/Q^2 = k_2^2/Q^2 \to 0$: in this limit logarithms appear which build up the anomalous dimension. They will be studied in the next section.

Next we now turn to D_3. The infrared finiteness follows from eqs.(3.1) and (3.2) which express, for both signature assignments, the D_3's in terms of the infrared finite D_2 amplitude. These equations also specify the behavior of D_3 at zero external momenta. For example, as $k_2 \to 0$:

$$D_3^{(-)}(k_1,k_2,k_3;\omega) \to g\frac{\sqrt{3}}{2}D_2(k_1,k_3;\omega), \tag{4.5}$$

whereas

$$D_3^{(-)}(k_1,k_2,k_3;\omega) = O(|k_1|) \tag{4.6}$$

as $k_1 \to 0$. Logarithms appear for $q^2=0$, as

$$k_1 = -k_2 - k_3 \to 0. \tag{4.7}$$

Let us now turn to D_4 and eqs.(2.10) - (2.12). Because of eqs.(3.3), (3.4), and (3.12) - (3.13) we can restrict ourselves to the even-signature case. We proceed in the same way as for D_2, i.e. we rewrite the integral equations as recursion relations. They are of the form (ignoring, for the moment, coefficients and the matrix structure of the equation):

$$D_{4,n+1} = D_{2,n}\otimes K_{2\to 4} + D_{3,n}\otimes\sum K_{2\to 3} + D_{4,n}\otimes\sum[K_{2\to 2} + \alpha - 1]. \tag{4.8}$$

Details follow from (2.10) - (2.12). The infrared finiteness has to be shown for each term seperately. We begin with the first term. First one remembers that D_2 has already been shown to be free from infrared singularities (and to vanish as its external momenta go to zero). When convoluting D_2 with $K_{2\to 4}$, the following integral arises:

$$\begin{aligned} g^4 &\int \frac{d^2k'}{(2\pi)^3} D_2(k',q-k';\omega)\frac{1}{k'^2(q-k')^2} \\ &\left(-q^2 + \frac{(k_1+k_2+k_3)^2(q-k')^2}{(q-k'-k_4)^2} + \frac{(k_2+k_3+k_4)^2k'^2}{(k'-k_1)^2} - \frac{k'^2(k_2+k_3)^2(q-k')^2}{(k'-k_1)^2(q-k'-k_4)^2}\right). \end{aligned} \tag{4.9}$$

We denote the four terms by a,b,c,d, resp., and look at the potentially dangerous regions of integration. All external momenta are taken to be nonzero. Near $k' = 0$ we combine terms "a" and "b" (both "c" and "d" are harmless), and near $k' = q$ we combine "a" and "c": the zeroes in the denominator are compensated. At $k' = k_1$ terms "c" and "d" have to be taken together, and at $k' = q - k_4 = k_1 + k_2 + k_3$ terms "b" and "d". Finally, when $q^2 = 0$ term "a" is absent. But the integral remains finite because the poles at $k'^2 = 0$ and $(q - k')^2 = 0$ are cancelled by the zeroes of D_2. This proves the absence of divergences in the first term of (4.8).

The next term in (4.8) involves integrals of a very similar type:

$$g^3 \int \frac{d^2k'}{(2\pi)^3} D_2(k', q_{123} - k', k_4; \omega) \frac{1}{k'^2(q_{123} - k')^2}$$
$$\left(-q_{123}^2 + \frac{(k_1 + k_2)^2 (q_{123} - k')^2}{(q_{123} - k' - k_3)^2} + \frac{(k_2 + k_3)^2 k'^2}{(k' - k_1)^2} - \frac{k'^2 k_2^2 (q_{123} - k')^2}{(k' - k_1)^2 (q_{123} - k' - k_3)^2} \right). \quad (4.10)$$

where $q_{123} = k_1 + k_2 + k_3$. Here the pattern of cancellations is the same as in (4.9). Now the case $q_{123} = 0$ leads to logarithmic factors, but they belong to anomalous dimensions which will be discussed in the following section. Finally we turn to the last term in eq.(4.8): now it is necessary to take a closer look at the numerical coefficients in eq.(2.11). One finds that each element of the 5×5 matrix can be written in such a way that it contains only combinations of the from (4.4). As an example, consider the (2,2) element:

$$-\frac{3}{2}(K_{2\to 2}(k_1, k_2) + K_{2\to 2}(k_3, k_4) + \alpha(k_1) + \alpha(k_2) + \alpha(k_3) + \alpha(k_4) - 4)$$
$$-\frac{3}{4}(K_{2\to 2}(k_1, k_4) + K_{2\to 2}(k_2, k_3) + K_{2\to 2}(k_1, k_3) + K_{2\to 2}(k_2, k_4)) =$$
$$-\frac{3}{2}K_{2\to 2}(k_1, k_2) + \frac{1}{2}[\alpha(k_1) + \alpha(k_2) - 2] - \frac{3}{2}K_{2\to 2}(k_3, k_4) + \frac{1}{2}[\alpha(k_3) + \alpha(k_4) - 2]$$
$$-\frac{3}{4}K_{2\to 2}(k_1, k_4) + \frac{1}{4}[\alpha(k_1) + \alpha(k_4) - 2] - \frac{3}{4}K_{2\to 2}(k_2, k_3) + \frac{1}{4}[\alpha(k_2) + \alpha(k_3) - 2]$$
$$-\frac{3}{4}K_{2\to 2}(k_1, k_3) + \frac{1}{4}[\alpha(k_1) + \alpha(k_3) - 2] - \frac{3}{4}K_{2\to 2}(k_2, k_4) + \frac{1}{4}[\alpha(k_2) + \alpha(k_4) - 2]. \quad (4.11)$$

Consequently, all divergencies cancel.

This completes our proof that all integrals on the rhs of (4.8) are finite in the infrared region, at fixed nonzero external momenta. What remains to be discussed in this section is the behavior in the external momenta k_1, k_2, k_3, k_4 (except for possible logarithmic factors which give rise to anomalous dimensions and will be investigated in the following section). In addition to eqs.(3.1) and (3.2), we need the following properties of the kernels (2.1) - (2.3):

$$K_{2\to 2}(k_1, k_2, k_1', k_2') \to 0, \quad (4.12)$$

as any of the four momenta goes to zero.

$$K_{2\to 3}(k_1, k_2, k_1', k_2', k_3') \to 0, \quad (4.13)$$

as any of the momenta (except for k_2') goes to zero, and

$$K_{2\to 3}(k_1, k_2, k_1', k_2', k_3') \to -g \cdot K_{2\to 2}(k_1, k_2, k_1', k_3'), \quad (4.14)$$

as $k_2' \to 0$. Finally:

$$K_{2\to 4}(k_1, k_2, k_1', k_2', k_3', k_4') \to 0, \quad (4.15)$$

as one of the momenta k_1, k_2, k_1', k_4' goes to zero, and

$$K_{2\to 4}(k_1, k_2, k_1', k_2', k_3', k_4') \to -g \cdot K_{2\to 3}(k_1, k_2, k_1', k_3', k_4'), \quad (4.16)$$

as $k_2' \to 0$.

With these properties we turn to the integral equation for the $D_{(4;R)}^{(++)}$ and take the limit $k_1 \to 0$. After some lengthy algebra one verifies that

$$D_{(4;R)}^{(C;++)}(\omega; k_1, k_2, k_3, k_4) \to 0 \quad (4.17)$$

for all color states. It is important to note that this property holds, in the antisymmetric color octet state, only for the "reduced" $D_{(4;R)}$ amplitude, not for the full D_4: this is why we had to subtract off the reggeization pieces $D_{(4;2-cut)}$. In the singlet and symmetric octet state, on the other hand, the property (4.16) holds for both D_4 and $D_{(4;R)}$, and we could use either amplitude (or a linear combination of them) for studying the deep inelastic limit.

5 Deep Inelastic Scattering

In this section we consider the "deep inelastic limit" of our D_4 amplitudes, i.e. the limit in which the photon mass Q^2 is much larger than any of the lower momenta k_1, k_2, k_3, k_4. What we wish to obtain is the singular (as the moment index $n \to 1$) piece of the twist-four four-gluon operator, i.e. both the anomalous dimension and the coefficient function. We are then facing the following general difficulty. From our previous discussion of the "solutions" of our integral equations we already know that our D_4 amplitudes contain, because of the reggeization of the gluon, pieces which have only two-reggeon cuts. They have the same form as the BFKL ladders, and their operator-product expansion starts with a twist-two term (see below). Compared to the D_2 amplitude, there is an

additional power of g^2 which is not compensated by a power of $\ln k^2/Q^2$: in this sense we are dealing with a nonleading correction to the twist-two term in the operator product expansion which we are going to ignore. What will interest us, are the twist-four pieces only. More generally, we will have to remove all nonleading twist-two pieces from our D_4 amplitudes, before we can start to discuss twist-four contributions. We then will find again a simple pattern: isolating the pieces with the maximal power of $\ln k^2/Q^2$, we find the ladder structure illustrated in Fig,4b. Moving from the bottom to the top, we have strong ordering of the the transverse momenta (and the virtualities), and the transition from the two-gluon to the four-gluon state defines a certain vertex function. Below this vertex the Q^2 evolution is described by a new anomalous dimension which we identify as the "four gluon anomalous dimension". Above the vertex, the Q^2 dependence is given by the anomalous dimension of the twist-four term of the BFKL ladder: numerically it is identical to the anomalous dimension of the leading twist-two term. Putting these three pieces together, we see a mixing pattern emerging between the four-gluon state and a nonleading piece of the two-gluon state: the anomalous dimensions do not mix, but the coefficient function does. As we shall point out further below, this is in disagreement with the GLR eqation.

We shall present our analysis in three steps: starting from the fermion loop at the top of Fig.4b, we first discuss the two-gluon state, in the limit where the momenta at the upper end are much larger than the lower ones. The main point is the expansion of the BFKL-Pomeron in powers of k^2/Q^2 and the anomalous dimensions associated with it. Next, we adress the transition vertex between the two-gluon and the four-gluon state and illustrate how the particular form of the vertex function couples the different terms in the expansion of D_2: in order to obtain the maximal number of powers of transerse logarithms, we are forced to consider the first nonleading term in D_2. Finally, we discuss the four-gluon state below this transition vertex and calculate the anomalous dimension of the four gluon operator. We also relate or results to short distance limits in configuration space.

5.1 The two-gluon state

Let us return to the two-gluon amplitude D_2 and its recursion relation eq.(4.2). In the previous section we discussed the cancellation of infrared singularites, avoiding the situation where all momenta $q^2, k^2, (q-k)^2$ are simultaneously small. But this is just the case where the short distance behavior is probed and will be the subject of this section. So let us first take $q = 0$, then $k^2 \to 0$. For the inhomogeneous term, eq.(4.1) is replaced by (2.6), and in the kernel (4.3) the first term $-3q^2$ is absent. All other terms have a factor k^2, so the whole expression is proportional to k^2.

A careful study, however, shows that the k' integral becomes logarithmically divergent as $k^2 \to 0$. This logarithm comes from the region of integration where $k^2 \ll k'^2 \ll Q^2$, and is correctly obtained if in (4.3) we approximate the kernel by:

$$-3\frac{g^2}{\omega}\int \frac{d^2k'}{(2\pi)^3} D_{2,n}(k',-k';\omega)\frac{1}{(k'^2)^2}\frac{-2k^2k'^2}{(k-k')^2}$$
$$\approx 3\frac{\alpha_s}{\omega\pi} const \int_{k^2}^{Q^2}\frac{dk'^2}{k'^2}\frac{(\frac{3\alpha_s}{\pi\omega}\ln Q^2/k^2)^n}{n!}, \qquad (5.1)$$

(where we have already assumed that from previous steps of iteration the small-k^2 behaviour is given by:

$$D_{2,n}(k,k;\omega) = const\cdot k^2(\frac{(\frac{3\alpha_s}{\pi\omega}\ln Q^2/k^2)^n}{n!}). \qquad (5.2)$$

The integral then results in

$$D_{2,n+1}(k,k;\omega) = const\cdot\frac{3\alpha_s}{\pi\omega}\cdot k^2\frac{(\frac{3\alpha_s}{\pi}\ln Q^2/k^2)^{n+1}}{(n+1)!}, \qquad (5.3)$$

instead of (4.1). When iterating (4.2) and taking the sum over n, it is convenient to write D_2 as a Mellin integral:

$$D_2(k,-k;\omega) = \int\frac{d\nu}{2\pi i}\tilde{D}(\nu,\omega)(\frac{k^2}{Q^2})^{1-\nu}, \qquad (5.4)$$

where the ν-contour runs along the imaginary axis with real part between zero and 1. For small k^2/Q^2 we are interested in the singularities in the ν-plane to the left of the contour: the nearest one lies near $\nu = 0$ at

$$\nu = \gamma_2(\omega) = \frac{3\alpha_s}{\omega\pi}. \qquad (5.5)$$

These logarithms, therefore, are the origin of the singular (in ω) part of the anomalous dimension of the two-gluon operator.

This pole near $\nu = 0$, however, is only the first of an infinite string of poles which are located near all negative integers (in fact, there are singularites also at half-integer values, but they depend upon the angle between the vectors Q and k and drop out if we restrict ourselves to angle-averaged amplitudes). This follows from the fact that there exists a complete set of eigenfunctions (all momenta are taken in units of $\sqrt{Q^2}$)

$$\chi_{n,\mu}(\mathbf{k}') = \frac{1}{\sqrt{2\pi}}e^{in\theta}(\mathbf{k}'^2)^{-1/2+i\mu}, \qquad (5.6)$$

of the forward BFKL kernel (4.4) (multiplied by $1/k^2k'^2$). This allows to write D_2 as:

$$D_2(k,-k;\omega) = k^2\sum_n\int d\mu\frac{\chi_{\mu,n}(\mathbf{k})}{1-\chi(\mu,n)}\int d^2\mathbf{k}'\chi^*_{\mu,n}(\mathbf{k}')\frac{1}{k'^2}D_{2;0}(k',-k';\omega), \qquad (5.7)$$

and the singularities in the μ-plane can be read off from the analytic form of the eigenvalue function:

$$\chi(n,\mu) = \frac{N_c\alpha_s}{\omega\pi}\left(2\psi(1) - \psi(\frac{1+n}{2}+i\mu) - \psi(\frac{1+n}{2}-i\mu)\right). \tag{5.8}$$

(where n is an integer, $-\infty < \mu < \infty$, and $\psi(x) = \frac{d\Gamma(x)}{dx}$). To leading order in g^2 the poles are found at:

$$\begin{aligned} -\frac{1}{2} + i\mu &= l - \gamma_2^{(l)}(\omega) \\ &= l - \frac{3}{\omega}\frac{\alpha_s}{\pi} \end{aligned} \tag{5.9}$$

with $l = 0, 1, 2, ...$ Note that the $\gamma_2^{(l)}$ are independent of l. This leads to the "twist" expansion of D_2:

$$D_2(k,-k;\omega) = \sum_l (\frac{k^2}{Q^2})^{(l+1-\gamma_2^{(l)}(\omega))} \sum_{k=0}^{l} C_{lk} e^{-ik\theta}. \tag{5.10}$$

In the ν-representation (5.4), the l-th term (for n=0) has the form:

$$\tilde{D}(\nu,\omega) \sim \frac{const}{\omega(\nu+l) - \frac{3\alpha_s}{\pi}}, \tag{5.11}$$

where the *const* has to be taken from the corresponding term in the twist-expansion of the inhomogeneous term $D_{(2;0)}$ in (2.6).

It is instructive to ask whether the next-to-leading term ($l = 1, n = 0$) in this expansion (which in (5.4) corresponds to the pole near $\nu = -1$) can also be found directly in momentum space. The affirmative answer is obtained if we look at the eigenvalue equation near $\nu = -1$:

$$\frac{6g^2}{\omega}k^2 \int \frac{d^2k'}{(2\pi)^3}\frac{1}{(k'^2)^2}\frac{k'^2}{(k-k')^2}(k'^2)^{1-\nu}. \tag{5.12}$$

The momentum integral is defined only for $0 < \Re\nu < 1$; the logarithmic divergence near $\nu = 0$ belongs to what we have discussed above, and the only way to reach $\Re\nu < 0$ is by analytic continuation. Formally, this is done by changing from k'^2 to $1/k'^2$ and integrating by parts. One then reaches the point $\nu = -1$ where again the integration diverges logarithmically. The correct coefficient of this logarithm is obtained if we expand the kernel in (5.12) in powers of k^2/k'^2 and retain the next-to leading term. This then allows to calculate the full next-to-leading term in (5.4) or (5.10): write the integral equation for D_2, expand the kernel in the way we have just outlined, and then impose strong ordering of the momenta. This procedure correctly reproduces the maximal number of transverse logs, i.e.the anomalous dimension.

Before we move on to the next part, the vertex function, we still have to mention one generalization of the BFKL ladder diagrams. We consider that part of the phase space in which the momenta

are strongly ordered (which, as we know, leads to the anomalous dimension of the leading-twist term). At the upper (large virtuality Q^2) end of the ladder graphs, we must have (opposite) equal momenta on both sides, otherwise we would not have found any logarithmic factors. At the lower (much smaller virtualities k_i^2) end, however, we might want to allow for slightly different k_1^2 and k_2^2 (the difference being still much smaller than Q^2). For this case it can be shown that we still find logarithmic divergences, but the argument is now changed to:

$$k^2(\ln Q^2/k^2)^n \to k_1 \cdot k_2(\ln Q^2/max(k_1^2,k_2^2))^n. \tag{5.13}$$

This feature will be used when we investigate the four-gluon state.

5.2 The transition vertex

The next step is the calculation of the transition vertex: two-gluon → four gluons. To this end we use the ν -representation (5.4) for the two-gluon amplitude and consider the momentum loop just above the transition from the two-gluon state to the four-gluon state (Fig.5). As an example, we write the full expression for the transition vertex which has been defined in (3.11) for the color singlet state (even signature). It contains both "connected" and the "disconnected" pieces. They are shown in Fig.5b and Fig.5c, resp., in the same order as written in (3.11). With the abreviations:

$$P(1;234) = g \cdot \frac{k^2}{(k-k_1)^2} K_{2\to3}(k_2,k_3,k_4), \tag{5.14}$$

$$Q(1;23;4) = g^2 \cdot \frac{k^2}{(k-k_1)^2}\left(K_{2\to2}(k_2,k_3) - \frac{1}{3}(\alpha(k_3)+\alpha(k_3)-\ldots)\right)\frac{k^2}{(k-k_4)^2}, \tag{5.15}$$

and

$$R(12;34) = g^2 \cdot \tilde{K}_{2\to2}(k_1,k_2)\frac{k^2}{(k-k_1-k_2)^2} \tag{5.16}$$

we have for the connected part $V^{(1)}(k;k_1,k_2,k_3,k_4)$ of the color singlet case:

$$\begin{aligned} &\frac{9}{\sqrt{8}}K_{2\to4}(\{k_1,k_2\}\{k_3,k_4\}) \\ &+\frac{9}{4\sqrt{8}}(P(2;431)+P(3;124)+P(4;123)+P(1;432)+ \\ &\qquad P(3;214)+P(4;213)+P(2;341)+P(1;342)) \\ &-\frac{\sqrt{2}g^2}{k^4}\left(\tilde{K}_{2\to2}(k_1,k_2+k_3+k_4)+\tilde{K}_{2\to2}(k_2,k_1+k_3+k_4)+\tilde{K}_{2\to2}(k_3,k_1+k_2+k_4)\right. \\ &\qquad +\tilde{K}_{2\to2}(k_4,k_1+k_2+k_3)-\tilde{K}_{2\to2}(k_1+k_2,k_3+k_4)-\tilde{K}_{2\to2}(k_1+k_3,k_2+k_4) \\ &\qquad \left.-\tilde{K}_{2\to2}(k_1+k_4,k_2+k_3)\right) \end{aligned}$$

$$+\sqrt{2}\,(R(12;34)+R(21;34)+R(34;12)+R(43;12)$$
$$-Q(3;12;4)-Q(4;12;3)-Q(1;34;2)-Q(1;43;2))$$
$$+\frac{9}{4\sqrt{8}}\,(Q(3;14;2)+Q(1;32;4)+Q(4;13;2)+Q(1;42;3).) \qquad (5.17)$$

(note that the symmetrization symbol in the arguments of $K_{2\to4}$ include a factor $\frac{1}{2^3}$; for simplicity we have put: $\tilde{K}_{2\to2}(k_1,k_2)=K_{2\to2}(k_1,k_2)-\frac{1}{3}(\alpha(k_1)+\alpha(k_2)-2)$). For the other color channels we have similar expressions which we shall not write down explicitly.

We are interested in the maximal number of logarithms, and we expect such a log to come from the region of integration where the $k^2\gg k_i^2$. We therefore expand the expressions given in (5.17) in powers of $\frac{\mathbf{k}_i\cdot\mathbf{k}_j}{k^2}$. This has to be done seperately for the connected and for the disconnected terms. The algebra is somewhat lengthy and will not be described in detail. The most striking result is that the leading terms cancel. The first nonvanishing contributions are therefore of the order k_i^4/k^4. In detail, we find:

$V^{(1)}(k;k_1,k_2,k_3,k_4)$:

$$-14\sqrt{2}\frac{\mathbf{k}_1\cdot\mathbf{k}_2\,\mathbf{k}_3\cdot\mathbf{k}_4}{k^2}+8\sqrt{2}\frac{\mathbf{k}_1\cdot\mathbf{k}_3\,\mathbf{k}_2\cdot\mathbf{k}_4+\mathbf{k}_1\cdot\mathbf{k}_4\,\mathbf{k}_2\cdot\mathbf{k}_3}{k^2} \qquad (5.18)$$

$V^{(8s)}(k;k_1,k_2,k_3,k_4)$:

$$-24\frac{\mathbf{k}_1\cdot\mathbf{k}_2\,\mathbf{k}_3\cdot\mathbf{k}_4}{k^2}+20\frac{\mathbf{k}_1\cdot\mathbf{k}_3\,\mathbf{k}_2\cdot\mathbf{k}_4+\mathbf{k}_1\cdot\mathbf{k}_4\,\mathbf{k}_2\cdot\mathbf{k}_3}{k^2} \qquad (5.19)$$

$V^{(27)}(k;k_1,k_2,k_3,k_4)$:

$$-36\sqrt{\frac{3}{2}}\frac{\mathbf{k}_1\cdot\mathbf{k}_2\,\mathbf{k}_3\cdot\mathbf{k}_4}{k^2} \qquad (5.20)$$

$V^{(8a)}(k;k_1,k_2,k_3,k_4)$:

$$-8\frac{\mathbf{k}_1\cdot\mathbf{k}_3\,\mathbf{k}_2\cdot\mathbf{k}_4-\mathbf{k}_1\cdot\mathbf{k}_4\,\mathbf{k}_2\cdot\mathbf{k}_3}{k^2} \qquad (5.21)$$

$V^{(10+\overline{10})}(k;k_1,k_2,k_3,k_4)$:

$$-8\sqrt{\frac{5}{2}}\frac{\mathbf{k}_1\cdot\mathbf{k}_3\,\mathbf{k}_2\cdot\mathbf{k}_4-\mathbf{k}_1\cdot\mathbf{k}_4\,\mathbf{k}_2\cdot\mathbf{k}_3}{k^2}. \qquad (5.22)$$

Combining these expressions with the two gluon propagators and the leading-twist of D_2 from above, we seem to have arrived at an integral of the type $d^2k/(k^2)^2$ which is infrared linear divergent. But since the expression for the full D_4 amplitude from which we have started had no such

divergence, this cannot be correct. In order to find the correct answer, we shall analyse the vertex in the same manner as we did with the nonleading terms of the two-gluon state. Namely use the Mellin representation (5.4) for the D_2 function above the vertex, and consider the whole expression as a function of ν. For each individual term $\mathbf{k}_i\cdot\mathbf{k}_j$ of the vertex function we find the usual logarithmic divergence at $\nu=0$ which produces the additional factor $1/\nu$. However, when adding up all the pieces, the residue of this ν-pole cancels and the k'-integral gives a finite contribution. Hence we are loosing a power of a transverse logarithm, and we interpret the remainder as a finite nonleading (with respect to $\ln Q^2/k^2$) correction to the twist-two operator. Disregarding for the moment this contribution, we move on to the next pole at $\nu=-1$. Technically this is done in the way described above (after (5.12)), namely by partial integration and continuation in ν. We then find a divergent behaviour at $\nu=-1$, and the logarithm is correctly obtained by expanding the integrand and keeping the terms proportional to k_i^4/k^4, (5.18)-(5.22). But as a result of taking twist-four of the ladder above, we have the additional power of k^2, and the dk^2/k^4, has turned into a logarithmic divergence. Since thislogarithm has its origin in strong ordering of transverse momenta, this pole near $\nu=-1$ may even allow a partonic interpretation. Counting powers in Q^2, the whole expression is proportional to $1/Q^4$.

So far we have discussed only the connected part of the vertex. For the disconnected part we have to calculate the vertexfunctions illustrated in Fig.5c, i.e.single loop contributions. They exhibit logarithmic divergencies, but a careful analysis shows that these logarithms always cancel among each other. Their contribution to the transition vertex, therefore, always looses one power of logarithms and hence has to be counted as nonleading. Details will be published elsewhere [23].

We conclude this subsection with the following remark. Instead of the equation (3.11), we could have used a slight modification of it. As we have discussed before, in the color 8_A channel, we where forced to subtract the piece $D_{(4;2-cut)}$ in order to obain the correct behaviour for small momenta. We then extended this subtraction procedure also to the other channels, 1 and 8_S; as a result, for the remaining amplitudes $D_{(4;R)}$ there is no direct coupling of the four-gluon state to the fermion loop. However, for the 1 and 8_S state this subtraction was not really necessary and we could have used a "mixed" form: in this case, the direct coupling of the four-gluon state to the fermion loop would appear in (3.11), and the transition vertex would have taken a different form. The final answer for the deep-inelastic behaviour, of course, remains the same.

5.3 The anomalous dimension of the four gluon operator

In this third part we calculate the anomalous dimension of the four- gluon operator. We want to calculate the diagrams illustrated in Fig.6 in the limit where $\frac{k_i^2}{Q^2} \ll 1$ for all i. For the vertex at the top of the diagrams and the momentum loop abov the vertex we know from the previous section that it consists of the three terms:

$$V(k;k_1,k_2,k_3,k_4) = \frac{g^4}{8\pi^2\omega(\nu+1)}\left(a_{(12)(34)}\mathbf{k}_1\cdot\mathbf{k}_2\,\mathbf{k}_3\cdot\mathbf{k}_4 + a_{(13)(24)}\mathbf{k}_1\cdot\mathbf{k}_3\,\mathbf{k}_2\cdot\mathbf{k}_4 + a_{(14)(23)}\mathbf{k}_1\cdot\mathbf{k}_4\,\mathbf{k}_2\cdot\mathbf{k}_3\right), \quad (5.23)$$

where the coefficients follow from (5.18) - (5.22) and depend upon the color assignment, and the factors in front result from loop above the vertex. In fact, we expet that our full amplitude will consist of three pieces:

$$T(k_1,k_2,k_3,k_4;\omega) = T_{(12)(34)}(k_1,k_2,k_3,k_4;\omega) + T_{(13)(24)}(k_1,k_2,k_3,k_4;\omega) + T_{(14)(23)}(k_1,k_2,k_3,k_4;\omega) \quad (5.24)$$

(each term also carries a color label which we have omitted). This decomposition follows from the structure of the diagrams that we wish to sum. Namely, from the integral equations (2.10) - 2.12) it follows that the amplitude can be written as:

$$T = T_0 + K\otimes T \quad (5.25)$$

with K denoting the sum of pairwise interactions:

$$K = K_{12} + K_{13} + K_{14} + K_{23} + K_{24} + K_{34}. \quad (5.26)$$

(in an obvious notation). However, it is more convenient to rearrange the sum: first define auxiliary "potentials" $\tilde{T}$ which denote the sum of all diagrams where only lines 1 and 2 or lines 3 and 4 interact:

$$\tilde{T}_{(12)(34)} = K_{12} + K_{34} + (K_{12}+K_{34})\otimes\tilde{T}_{(12)(34)}. \quad (5.27)$$

Similarly, we define $\tilde{T}_{(13)(24)}$ and $\tilde{T}_{(14)(23)}$. The full amplitude can then be written as:

$$T = T_{(12)(34)} + T_{(13)(24)} + T_{(14)(23)} \quad (5.28)$$

with

$$\begin{pmatrix} T_{(12)(34)} \\ T_{(13)(24)} \\ T_{(14)(23)} \end{pmatrix} =$$

$$\begin{pmatrix} T_{(12)(34);0} \\ T_{(13)(24);0} \\ T_{(14)(23);0} \end{pmatrix} + \begin{pmatrix} \tilde{T}_{(12)(34)} & 0 & 0 \\ 0 & \tilde{T}_{(13)(24)} & 0 \\ 0 & 0 & \tilde{T}_{(14)(23)} \end{pmatrix}\cdot\begin{pmatrix} 0&1&1\\1&0&1\\1&1&0 \end{pmatrix}\begin{pmatrix} T_{(12)(34)} \\ T_{(13)(24)} \\ T_{(14)(23)} \end{pmatrix}. \quad (5.29)$$

Here we have defined:

$$\begin{pmatrix} T_{(12)(34);0} \\ T_{(13)(24);0} \\ T_{(14)(23);0} \end{pmatrix} = \begin{pmatrix} \tilde{T}_{(12)(34)} & 0 & 0 \\ 0 & \tilde{T}_{(13)(24)} & 0 \\ 0 & 0 & \tilde{T}_{(14)(23)} \end{pmatrix}\cdot\left(\begin{pmatrix} 1&0&0\\0&1&0\\0&0&1 \end{pmatrix} + \frac{1}{2}\begin{pmatrix} 0&1&1\\1&0&1\\1&1&0 \end{pmatrix}\right)\begin{pmatrix} V_{(12)(34)} \\ V_{(13)(24)} \\ V_{(14)(23)} \end{pmatrix}, \quad (5.30)$$

where the vector V consists of the three terms in (5.22) (the factor $\frac{1}{2}$ in the inhomogeneous term results from the angular integration and will be explained further below). As a result, the decomposition (5.24) holds.

To make this equation complete, we have to reintroduce the color degrees of freedom. The integral equations (2.10 - 12) have been written for the color-coupling scheme (12)(34). When discussing infrared finiteness, we showed that the trajectory functions in the four- gluon state can always be distributed in such a way that kernel $K_{2\to 2}$ plus trajectory functions come in the infrared finite combination (4.4) (or a multiple of it). So from now on we absorbe the trajectory functions into the kernel and define an "effective" kernel. Since, for this section, we have decided to reorganize the sum of diagrams, it is more convenient to use other color coupling schemes. For example, for $\tilde{T}_{(13)(24)}$ in (5.29) (defined in analogy with (5.27)) it is most natural to use the (13)(24) coupling scheme, rather than (12)(34). Proceeding this way, each rung inside a ladder comes with one of the color factors $(-3,-\frac{3}{2},-\frac{3}{2},0,1)$ for C=$(1,8_A,8_S,10+\overline{10},27)$, resp. Furthermore, at the transition from $\tilde{T}_{(12)(34)}$ to $\tilde{T}_{(13)(24)}$ we then have to insert the recoupling matrix A (see eq.(A.17)) which translates from one color basis to another. Inserting these recoupling matrices into (5.29), we arrive at a vector equation with 15 components, and the matrix on the rhs of (5.29) turns into the 15×15 matrix S (for the explicit form see below). Furthermore, the vector V in (5.30) has, in its first five components, the color coefficients of the first term in (5.23), components 6 to 10 consist of the color coefficients of the second term in (5.23), multiplied by the matrix A^T, components 11 to 16 the coefficients of the third term in (5.23), multiplied with the matrix PA^TP.

Let us now study how the transverse logarithms arise. We begin at the top with the vertex (5.23). Above the vertex we have (5.4) for D_2, and from the discussion above we have learned that we are interested in the point $\nu=-1$, rather than the leading pole at $\nu=0$. It will be convenient

to introduce $\tilde{\nu} = \nu + 1$, such that the point of interest lies again at $\tilde{\nu} = 0$. For the vertex we have the expressions (5.23), derived in the previous subsection.

Now put two ladders underneath (Fig.7a), e.g. $\tilde{T}_{(12)(34)}$. In each ladder with color i, a rung gives one power of a logarithm and preserves the structure $\mathbf{k_i} \cdot \mathbf{k_j}$ ((5.12)). Therefore the result in the $(\omega, \tilde{\nu})$ representation reads:

$$\mathbf{k_1} \cdot \mathbf{k_2} \mathbf{k_3} \cdot \mathbf{k_4} \cdot \int\int \frac{d\tilde{\nu}_1}{2\pi i} \frac{d\omega_1}{2\pi i} e^{\tilde{\nu}_1 \ln Q^2/max(k_1^2,k_2^2)} e^{(\tilde{\nu}-\tilde{\nu}_1)\ln Q^2/max(k_3^2,k_4^2)} \frac{\frac{a_i}{\tilde{\nu}_1} + \frac{a_j}{(\tilde{\nu}-\tilde{\nu}_1)}}{[\omega_1\tilde{\nu}_1 - a_i][(\omega-\omega_1)(\tilde{\nu}-\tilde{\nu}_1) - a_i]}. \tag{5.31}$$

Here we have omitted all contributions that come from the two-gluon system above or the vertex. Furthermore, we have put:

$$a_i = -c_i \frac{\alpha_s}{\pi}, \tag{5.32}$$

where c_i stands for one of the color factors: $(-3, -\frac{3}{2}, -\frac{3}{2}, 0, 1)$ for $(1, 8_A, 8_S, 10 + \overline{10}, 27)$, resp. If $max(k_1^2, k_2^2) = max(k_3^2, k_4^2) = k^2$, we can carry out the $\tilde{\nu}_1$-integral and obtain:

$$\mathbf{k_1} \cdot \mathbf{k_2} \mathbf{k_3} \cdot \mathbf{k_4} e^{\tilde{\nu} \ln Q^2/k^2} \left(\frac{1}{\sqrt{1 - 4a_i/\omega\tilde{\nu}}} - 1 \right). \tag{5.33}$$

Next we consider the "switch" (Fig.7b) to, say, $\tilde{T}_{(14)(23)}$, where for simplicity we include only one rung in each ladder below (color j). Note that logarithms are obtained only if the momentum transfer above the rung is much smaller then the virtualities of the vertical gluon lines. This forces the two upper ladders to have identical momenta at their lower end, and eq.(5.32) applies. Starting from the expression

$$c_i^2 g^4 \int \frac{d^2k d^2k'}{(2\pi)^6} \frac{2(\mathbf{k}\mathbf{k}')q_1^2}{k^2(k-q_1)^2} \frac{2(\mathbf{k}\mathbf{k}')q_2^2}{k'^2(k'-q_2)^2} e^{\tilde{\nu} \ln Q^2/max(k^2,k'^2)}, \tag{5.34}$$

one convinces oneself that logarithms are obtained if either $k^2 \ll k'^2$ or $k'^2 \ll k^2$. After the angular integration one obtains for the first region in (5.32) (for simplicity we take $q_1^2 = q_2^2 = q^2$):

$$\frac{1}{2} \left(q^2 \frac{c_j g^2}{4\pi^2 \omega} \right)^2 \int_{q^2}^{Q^2} \frac{dk'^2}{k'^2} \int_{q^2}^{k'^2} \frac{dk^2}{k^2} e^{\tilde{\nu} \ln Q^2/k'^2}. \tag{5.35}$$

A similar result holds for the second region. Note the factor $\frac{1}{2}$ in front, which results from the angular integration; the factor $\frac{1}{2}$ in (5.30) has the same origin. Including more rungs below and carrying out the summation leads to:

$$q^2 q^2 e^{\tilde{\nu} \ln Q^2 q^2} \left(\frac{1}{\sqrt{1 - 4a_i/\omega\tilde{\nu}}} - 1 \right) \left(\frac{1}{\sqrt{1 - 4a_j/\omega\tilde{\nu}}} - 1 \right). \tag{5.36}$$

If at the lower end the two ladders have the same momenta but are not in the forward direction (Fig.7b) we have to replace q^2 by $max(q^2, q'^2)$. If the two ladders at the lower end have different momenta $k_1, ..., k_4$, the last "propagator" in (5.34) has to be replaced by:

$$\left(\frac{1}{\sqrt{1 - 4a_j/\omega\tilde{\nu}}} - 1 \right) \to \int\int \frac{d\tilde{\nu}_1}{2\pi i} \frac{d\omega_1}{2\pi i} e^{\tilde{\nu}_1 \ln Q^2/max(k_1^2,k_2^2)} e^{(\tilde{\nu}-\tilde{\nu}_1)\ln Q^2/max(k_3^2,k_4^2)} \frac{\frac{a_i}{\tilde{\nu}_1} + \frac{a_j}{(\tilde{\nu}-\tilde{\nu}_1)}}{[\omega_1\tilde{\nu}_1 - a_j][(\omega-\omega_1)(\tilde{\nu}-\tilde{\nu}_1) - a_j]} \tag{5.37}$$

(cf.the discussion before eq.(5.33)).

Including more two-ladder states at the bottom, we obviously repeat the previous steps: for each two-ladder state we have a "propagator" (cf.eq.(5.33)), and at each "switch" we get the color recoupling matrix and the factor $\frac{1}{2}$.

We can make this more formal by stating the following rules for calculating the deep inelastic limit of the four gluon state (Fig.6). For completeness, we include also the results from the two-gluon state and the transition vertex. We use the $\tilde{\nu}$-representation, and for simplicity take all k_i^2 of the same order k^2. Then the amplitude is of the form:

$$\frac{-1}{Q^4} \int \frac{d\tilde{\nu}}{2\pi i} \tilde{D}_4(\omega, \tilde{\nu}) \left(\frac{k^2}{Q^2}\right)^{-\tilde{\nu}}, \tag{5.38}$$

where the overall minus sign has been discussed in section 2. $\tilde{D}_4$ will be constructed as follows:

(i) Starting with the two-gluon channel above, we have the "propagator" of eq.(5.11) with $l = 1$ and $\tilde{\nu} = \nu + 1$.

(ii) For the transition vertex, put the factor $\alpha_i^2 \cdot V^T$, where V is the vector obtained and described after (5.30).

(iii) For each two-ladder state below the vertex we have a propagator matrix

$$G = 1 \otimes diag \left(\left(\frac{1}{\sqrt{1 - 4a_1/\omega\tilde{\nu}}} - 1 \right), \left(\frac{1}{\sqrt{1 - 4a_2/\omega\tilde{\nu}}} - 1 \right), \left(\frac{1}{\sqrt{1 - 4a_3/\omega\tilde{\nu}}} - 1 \right), \left(\frac{1}{\sqrt{1 - 4a_4/\omega\tilde{\nu}}} - 1 \right), \left(\frac{1}{\sqrt{1 - 4a_5/\omega\tilde{\nu}}} - 1 \right) \right), \tag{5.39}$$

where the unity matrix is three dimensional. It is easily seen that the next-to-last element in the second matrix, which refers to the color channel $10 + \overline{10}$ vanishes: this can be used to reduce our 15×15 matrix to a 12×12 one.

(iv) At each switch, we have a color recoupling matrix and the factor $\frac{1}{2}$ from the angular integration. In our 15-dimensional space, this produces the matrix S which describes the "switching" and has

the form:

$$S = \begin{pmatrix} 0 & \Lambda & P\Lambda P \\ \Lambda^T & 0 & \Lambda^T P \Lambda P \\ P\Lambda^T P & P\Lambda^T P \Lambda & 0 \end{pmatrix}. \tag{5.40}$$

(v) Finally, summing over all repetitions of the two-ladder states, we obtain the geometric series:

$$\sum_{n=0}^{\infty} \left(G \frac{1}{2} S \right)^n G = \left(G^{-1} - \frac{1}{2} S \right)^{-1}. \tag{5.41}$$

(vi) At the lower end, multiply with the vector E:

$$E = \begin{pmatrix} \mathbf{k}_1 \cdot \mathbf{k}_2 \, \mathbf{k}_3 \cdot \mathbf{k}_4 \\ \Lambda \; \mathbf{k}_1 \cdot \mathbf{k}_3 \, \mathbf{k}_2 \cdot \mathbf{k}_4 \\ P\Lambda P \; \mathbf{k}_1 \cdot \mathbf{k}_4 \, \mathbf{k}_2 \cdot \mathbf{k}_3 \end{pmatrix}. \tag{5.42}$$

(note that in color space E is a matrix).

(vii) If the two ladders at the lower end have different momenta $k_1, ..., k_4$, the last propagator G on the lhs of (5.38) has to be replaced according to what has been said before (5.33).

Putting all this together, we have the following result:

$$D^{(i;++)}_{(4;R)} = \frac{1}{Q^4} \int \frac{d\tilde{\nu}}{2\pi i} \left(\frac{k^2}{Q^2} \right)^{-\tilde{\nu}} \frac{3}{40\pi} \frac{1}{\omega\tilde{\nu} - a_1} \frac{\alpha_s^2}{\omega\tilde{\nu}} V^T (G^{-1} - \frac{1}{2} S)^{-1} E. \tag{5.43}$$

Here the color superscript "i" refers to the color content the "last" two ladder state. In addition to this result, we still need to add (see eq.(3.9)) the pole terms at $\nu = -1$ of the $D_{(4;2-cut)}$ pieces, which have the same singularities in ν as D_2.

5.4 Discussion

When trying to evaluate the $\tilde{\nu}$-integral in (5.43), we first need to find, in the $\tilde{\nu}$-plane, the rightmost singularity in the four-gluon channel. A computer calculation leads to a pole at

$$\omega\tilde{\nu} = 12.1146 \frac{\alpha_s}{\pi}. \tag{5.44}$$

The state to which this singularity belongs is completely symmetric under exchanging (12)(34) with (13)(24) or (14)(23), and the ladders are mainly in a color singlet. To the left of this leading singularity, a branch cut starts at

$$\omega\tilde{\nu} = 12 \frac{\alpha_s}{\pi}. \tag{5.45}$$

Let us briefly discuss this result. As it can be seen from (5.31), the branch point (5.45) belongs to the two-ladder state (the ladders being in a color singlet each). The repetition of two-ladder

states (Fig.6) generates a pole slightly to the right of the branch point: the "switches" can be viewed as an "attractive interaction" between ladders. The weakness of this interaction can directly be traced back to color factors, suggesting that a $1/N_c$ expansion might give a simple picture.. This idea will be persued elsewhere. The whole situation resembles very much that of particle and bound state singularities of the S-matrix in the energy plane (Fig.8): a ladder corresponds to an "elementary particle" with "mass square"$= \frac{\alpha_1}{\omega} \frac{\alpha_s}{\pi}$, two ladders have their "threshold" at $4 \frac{\alpha_1}{\omega} \frac{\alpha_s}{\pi}$ etc. The new pole in (5.44) belongs to a "bound state" slightly to the right of the two-particle threshold. The language we have been using here refers more to a t-channel analysis. However, it should be possible to translate this "bound state" also into a s-channel picture.

Doing in (5.43) the $\tilde{\nu}$ integral, we have contributions from the two-gluon state and from the singularities in the four-gluon state. Symbolically:

$$D_{(4;R)} = A e^{\gamma_2^{(1)} \ln Q^2/k^2} + B e^{\gamma_4 \ln Q^2/k^2}, \tag{5.46}$$

whereas

$$D_{(4;2-cut)} = C exp^{\gamma_2^{(1)} \ln Q^2/k^2}. \tag{5.47}$$

Here $\gamma_2^{(1)}$ denotes the anomalous dimension of the twist-four piece of the two gluo . function (second term in the expansion eq.(5.10)), and γ_4 is the "bound state" pole of the four-gluon state (5.43).

When deriving this result we have seen that it is the particular structure of the transition vertex which couples the four-gluon state to the first nonleading term in D_2, rather than the leading one. There is no doubt that the leading term in the k^2/Q^2 expansion of the D_2 amplitude coincides with the short distance behaviour of the two-gluon operator. We expect this to be true also for the four gluon state for which we have analysed in the previous subsection the leading behaviour in $k_i^2/Q^2 \to 0$. This allows to identify $\gamma_2^{(0)}$ and γ_4 as the anomalous dimensions of the two-gluon and four-gluon operator, resp.. However, our D_2 amplitude also contains higher powers in k^2/Q^2, and their interpretation in terms of gluon field operators is less clear. Most likely, the first nonleading term belongs to a higher derivative of the two-gluon operator. We therefore interpret our result as a mixing beeween the four gluon operator (with twist 4) and a twist-four piece of the two-gluon operator. It is important to note that this mixing does not yet affect the anomalous dimensions but only the coefficent function: the matrix of anomalous dimensions obtained so far is half diagonal:

$$\gamma = \begin{pmatrix} \gamma_2 & 0 \\ \gamma_{24} & \gamma_4 \end{pmatrix}. \tag{5.48}$$

The off-diagonal element γ_{24} which comes from the trasnition vertex (5.23) is of order α_s^2. Because of the zero in the other off-diagonal element, it has no effect on the eigenvalues but only determines the eigenvectors. It is obvious that this matrix is not complete: what is missing is a study of the "inverse" of the transition vertex, the transition of the four-gluon state back to the two-gluon state. If this transition, again, gives the maximal power of transverse logarithms, the zero in (5.44) will be replaced by an expression of the order α_s^2. This gives a correction to the eigenvalues of the order α_s^2, and hence does not change the leading order results of this paper. Nevertheless, this missing element needs to be calculated.

Next, it may instructive to translate our momentum space considerations into configuration space. We first return to the two-gluon amplitude D_2. Following [12] we take the Fourier transform with respect to all four external transverse momenta. Denote the space vectors (impact parameter) by $\mathbf{R}_1, \mathbf{R}_2, \rho_1, \rho_2$ for the two photon and the two gluon lines, resp. Conservation of momenta is equivalent to translational invariance, and since the momentum transfer $(Q-Q)^2 = (k_1+k_2)^2$ is taken to be zero, we have only two independent space coordinates (impact parameter variables). We chose them to be the distance between to the two upper photon lines, $\mathbf{R}_{12}$ and the distance between the two gluon lines at the bottom $\rho_{12} = \frac{1}{\sqrt{2}}(\rho_1 - \rho_2)$. The limit $k^2 \ll Q^2$ is equivalent to $\mathbf{R}_{12}^2 \ll \rho_{12}^2$, i.e. what we have studied is really the short distance limit, and the expansion (5.4) is a short distance expansion.

Now let us try the same for D_4 (Fig.9). With the same arguments as before, we have four independent space vectors, which we choose to be $\mathbf{R}_{12}$, $\rho_{12} = \frac{1}{\sqrt{2}}(\rho_1 - \rho_2)$, $\rho_{34} = \frac{1}{\sqrt{2}}(\rho_3 - \rho_4)$, $\rho_{(12)(34)} = \frac{1}{2}(\rho_1 + \rho_2 - \rho_3 - \rho_4)$. The conjugate momenta are $\sqrt{2}\mathbf{Q}$, $\mathbf{k}_{12} = \frac{1}{\sqrt{2}}(\mathbf{k}_1 - \mathbf{k}_2)$, $\mathbf{k}_{34} = \frac{1}{\sqrt{2}}(\mathbf{k}_3 - \mathbf{k}_4)$, $\mathbf{k}_{(12)(34)} = \frac{1}{2}(\mathbf{k}_1 + \mathbf{k}_2 - \mathbf{k}_3 - \mathbf{k}_4)$. Now we have several options of defining short distance limits. For example, the limit

$$k_{(12)(34)}^2 \ll k_{12}^2 \ll k_{34}^2 \ll Q^2 \tag{5.49}$$

is equivalent to

$$R_{12}^2 \ll \rho_{34}^2 \ll \rho_{12}^2 \ll \rho_{(12)(34)}^2. \tag{5.50}$$

From our analysis in momentum space we see that the short distance behaviour in ρ_{12}^2 and ρ_{34}^2 is described by the anomalous dimension of the leading term of the two-gluon amplitude, whereas the behaviour in $\rho_{(12)(34)}$ is governed by the new anomalous dimension. All this indicates that D_4 allows for a multiple operator expansion.

We can use this language also in order to interpret the evolution of the four-gluon state. At each "switch" from one two-ladder state to another one we found that only certain parts of the region of integration are of importance, and we can translate this into configuration space. For example, if in Fig.9 we denote the variables at the upper end of the upper ladders by ρ_i', the variables at the "switch" by ρ_i'', and the variables at the bottom by ρ_i, one of the relevant orderings is:

$$\begin{aligned} R_{12}^2 &\ll \ldots \ll \\ &\ll \rho_{12}'^2 \ll \rho_{34}'^2 \\ &\ll \rho_{(12)(34)}'^2 \approx \rho_{14}''^2 \ll \rho_{23}''^2 \\ &\ll \rho_{(12)(34)}''^2 \approx \rho_{14}^2 \ll \rho_{23}^2 \\ &\ll \ldots \ll . \end{aligned} \tag{5.51}$$

Finally, we want to comment on the Gribov-Levin-Ryskin equation. The first point of discussion is the anomalous dimension of the four-gluon state [1]. This equation (more precisely: its second term, the first fan-diagram) contains only the state of two noninteracting ladders, which in the ν-plane gives rise to a square-root branch point. It misses the "switches" which are responsible for the new "bound state" pole. Although its position is very close to the "threshold" branch point, its presence will influence the size of the four-gluon correction to the GLAP-equation at given values of Bjorken-x and Q^2. The same will most likely be true for all the other fan diagrams in the GLR equation: each multi-gluon state will have its own "new bound state" to the right of the corresponding many-ladder threshold, whereas the GLR-equation misses this effect completely. By how much the GLR equation is misrepresenting QCD, is presently completely open: one of the questions to be clarified is how close to the "thresholds" are the "new bound states". Unfortunately, almost all numerical estimates of the "screening" corrections are based upon the GLR equation. This makes clear that theoretical work along this line is badly needed.

There is still another discrepancy between the present analysis and the GLR equation. It concerns the "mixing" between the two-gluon and the four-gluon state. We have made clear that the four-gluon state when combined with the leading-twist term of the two-gluon amplitude loses one power of transverse logarithms and hence must be counted as a nonleading contribution to the leading twist. If, on the other hand, the four-gluon state is combined with the twist-four term of the two-gluon amplitude, we find the maximal number of logarithms and have strong ordering

[1] The existence of the an anomalous dimension larger than than $12\frac{\alpha_s}{\omega_\pi}$ has been confirmed now [24] by the authors of the GLR equation. However, we do not agree with the numerical value.

all along the diagrams. In contrast to this, the first fan diagram of the GLR equation contains an integral d^2k/k^4 just above the transition vertex which is infrared divergent and hence needs a cutoff. For the two-gluon ladder above the vertex there exist two versions of the equation. In the so-called DLA-approximation, only the leading twist-two term is kept. In this case the GLR equation misses the mixing between the four gluon state and the twist-four term of the two-gluon ladder. In another version the full BFKL amplitude is used: in this case, as we believe, the k-integral is treated incorrectly.

A third discrepancy lies in the expression for the transition vertex: We do not agree with the result of [25].

6 Conclusions

In this paper we have analyzed the singular part of the (twist four) four-gluon operator. The motivation comes from the need to establish a solid background for analyzing within QCD the low-x region of deep inelastic scattering. We have computed the anomalous dimension of the four-gluon operator as well as the coefficient function; the latter consists of a fermion loop through which the photon couples to the two, three, and four-gluon states and the transition vertex from the two-gluon to the four gluon state. We find mixing between a twist-four piece of the BFKL-Pomeron and the four-gluon state; this mixing does not apply to the anomalous dimension but only to the coefficient function. Accordingly, there is some freedom in defining the transition vertex. The fact that the leading part of the twist-four four gluon operator comes from strongly ordered transerse momenta indicates that we might be able to give a partonic interpretation.

Very unfortunately, some of our results disagree with the GLR- equation which so far has been the only available tool for estimating the size of new effects in the low-x region. The first disagreement is in the anomalous dimension; this has been confirmed by now by the authors. In addition to that, however, we also do not agree with the way in which the GLR-equation treats the mixing between the two and the four gluon operator, and we find contributions to the transition vertex which have not been included in the GLR-equation. As a consequence, there is now uncertainty how reliable the numerical estimates based upon the GLR equation are. The fact that the difference in the anomalous dimension is found to be rather small gives some hope that the GLR equation may still be a decent approximation, but this needs to be clarified.

So far we do not know the magnitude of the corrections derived in this paper. The next step.

therefore, must be a numerical analysis based upon the given expressions. The strong ordering which we have just mentioned suggests that it may be possible to define a modified evolution scheme (which, however, will definitely differ from the GLR-equation). The main feature is that the evolution of the four-gluon state cannot be related in any simple way to the evolution of the two-gluon state. It is the new "bound state" which prevents such a simple situation. Consequently, we think that its appearance marks a real new physical effect in the parton picture. In order to obtain a more intuitive interpretation, one should try to understand this phenomenon in a s-channel language.

Acknowledgements: Helpful discussions with E.M.Levin, A.Mueller, M.Wuesthoff, and J.Blümlein are gratefully acknowledged.

A SU(3) TENSOR ALGEBRA

In this appendix we collect a few formula which are useful for the reduction of the SU(3) tensors. To a large extent we follow the procedure of I, but in order to keep the paper reasonably short, we limit ourselves to the color zero t-channel and do not consider t-channel configurations with other color quantum numbers. A useful compendium of SU(3) structure constants and their properties can be found in [26].

We begin with the $2 \to 2$ projection operators:

$$\begin{aligned}
P_1(a_1,b_1;a_2,b_2) &= \frac{1}{8}\delta_{a_1b_1}\delta_{a_2b_2} \\
P_{8_A}(a_1,b_1;a_2,b_2) &= \frac{1}{3}f_{a_1b_1c}f_{a_2b_2c} \\
P_{8_S}(a_1,b_1;a_2,b_2) &= \frac{3}{5}d_{a_1b_1c}d_{a_2b_2c} \\
P_{10+\bar{10}}(a_1,b_1;a_2,b_2) &= \frac{1}{2}(\delta_{a_1a_2}\delta_{b_1b_2}-\delta_{a_1b_2}\delta_{a_2b_1})-\frac{1}{3}f_{a_1b_1c}f_{a_2b_2c} \\
P_{27}(a_1,b_1;a_2,b_2) &= \frac{1}{2}(\delta_{a_1a_2}\delta_{b_1b_2}+\delta_{a_1b_2}\delta_{a_2b_1})-\frac{1}{8}\delta_{a_1b_1}\delta_{a_2b_2}-\frac{3}{5}d_{a_1b_1c}d_{a_2b_2c}
\end{aligned} \tag{A.1}$$

(note that we do not need to decompose the 10 and the $\bar{10}$ representations) These projectors satisfy:

$$P_C(a_1b_1;a_2b_2)P_{C'}(a_2b_2;a_3b_3) = \delta_{CC'}P_C(a_1b_1;a_3b_3) \tag{A.2}$$

with $C = 1, 8_A, 8_S, 10+\bar{10}, 27$. We shall also use the shorthand notation:

$$P_C P_{C'} = \delta_{CC'}P_C. \tag{A.3}$$

Another property is the completeness:

$$\sum_C P_C = 1. \tag{A.4}$$

With these projection operators we decompose the group factors $t_{2\to2}(a_1b_1;a_2b_2)$ of the kernel $K_{2\to2}$ in the integral equation (cf.(I,4.6)) into irreducible representations. With

$$t_{2\to2}(a_1b_1;a_2b_2) = f_{a_1ca_2}f_{cb_1b_2} \tag{A.5}$$

one obtains:

$$t_{2\to2} = -3P_1 - \frac{3}{2}P_{8_A} - \frac{3}{2}P_{8_S} + P_{27}. \tag{A.6}$$

Next we come to the case $2 \to 3$. Within the coupling scheme of Fig.x, we define normalized transition tensors $T_{C,C_{23}}$. The normalization is such that

$$T_{C,C_{23}} \cdot T_{C',C'_{23}} = \delta_{C,C'}\delta_{C_{23},C'_{23}} \cdot P_C. \tag{A.7}$$

We limit ourselves to two cases: $C = 1$ and $C = 8_A$. We begin with the color singlet t-channel. We then have only two possibilities: $C_{23} = 8_A$ and $C_{23} = 8_S$. The corresponding tensors are:

$$\begin{aligned}
T_{1,8_A}(a_1b_1a_2b_2c_2) &= \frac{1}{8\sqrt{3}}\delta_{a_1b_1}f_{a_2b_2c_2} \\
T_{1,8_S}(a_1b_1a_2b_2c_2) &= \frac{1}{8}\sqrt{\frac{3}{5}}\delta_{a_1b_1}d_{a_2b_2c_2}
\end{aligned} \tag{A.8}$$

It is then easy to analyse the group part $t_{2\to3}$ of the kernel $K_{2\to3}$, which is of the form:

$$t_{2\to3}(a_1b_1;a_2b_2c_2) = f_{a_1la_2}f_{lmb_2}f_{mb_1c_2}. \tag{A.9}$$

In the color zero channel we find

$$t_{2\to3} = \frac{3\sqrt{3}}{2}T_{1,8_A} \tag{A.10}$$

Since each pair of two lines is in the 8_A state, multiplication with the tensor $t_{\cdot,2}$ always gives a factor $-\frac{3}{2}$ (cf.eq.(A.6)).

Similarly the color octet channel $C = 8_A$. The normalized transition operators are:

$$\begin{aligned}
T_{8_A,1}(a_1b_1;a_2b_2c_2) &= \sqrt{\frac{8}{3}}f_{a_1b_1c}P_1(a_2m;b_2c_2) \\
T_{8_A,8_A}(a_1b_1;a_2b_2c_2) &= \frac{1}{\sqrt{3}}f_{a_1b_1c}P_{8_A}(a_2m;b_2c_2) \\
T_{8_A,8_S}(a_1b_1;a_2b_2c_2) &= \frac{1}{\sqrt{3}}f_{a_1b_1c}P_{8_S}(a_2m;b_2c_2) \\
T_{8_A,10+\bar{10}}(a_1b_1;a_2b_2c_2) &= \sqrt{\frac{2}{15}}f_{a_1b_1c}P_{10+\bar{10}}(a_2m;b_2c_2) \\
T_{8_A,27}(a_1b_1;a_2b_2c_2) &= \frac{2\sqrt{2}}{9}f_{a_1b_1c}P_{27}(a_2m;b_2c_2)
\end{aligned} \tag{A.11}$$

The decomposition of $t_{2\to3}$ in the 8_A channel yields:

$$t_{2\to3} = -3\sqrt{\frac{3}{8}}T_{8_A,1} - \frac{3\sqrt{3}}{4}T_{8_A,8_A} - \frac{3\sqrt{3}}{4}T_{8_A,8_S} - \frac{3}{2\sqrt{2}}T_{8_A,27}. \tag{A.12}$$

Finally the case $2 \to 4$. Here we have two coupling schemes (Fi.xa and b). For the sake of brevity we limit ourselves to the first one (Fig.xa): since the total color quantum number is zero,

the two subsytems (12) and (34) must have identical group assignments. We first define normalized transition operators $T_{2\to 4}$ which satisfy:

$$T_{C;C_{12},C_{34}} \cdot T_{C';C'_{12},C'_{34}} = \delta_{II'}\delta_{I_{12}I'_{12}}\delta_{I_{34}I'_{34}}P_I. \tag{A.13}$$

We have five possibilities. In components, these tensors are:

$$\begin{aligned}
T_{111}(a_1b_1;a_2b_2c_2d_2) &= \frac{1}{\sqrt{8}}\delta_{a_1b_1}P_0(b_2a_2;c_2d_2)\\
T_{18_A8_A}(a_1b_1;a_2b_2c_2d_2) &= \frac{1}{8}\delta_{a_1b_1}P_{8_A}(b_2a_2;c_2d_2)\\
T_{18_S8_S}(a_1b_1;a_2b_2c_2d_2) &= \frac{1}{8}\delta_{a_1b_1}P_{8_S}(b_2a_2;c_2d_2)\\
T_{1(10+\bar{10})(10+\bar{10})}(a_1b_1;a_2b_2c_2d_2) &= \frac{1}{4\sqrt{10}}\delta_{a_1b_1}P_{10}(b_2a_2;c_2d_2)\\
T_{1(27)(27)}(a_1b_1;a_2b_2c_2d_2) &= \frac{1}{6\sqrt{6}}\delta_{a_1b_1}P_{27}(b_2a_2;c_2d_2)
\end{aligned} \tag{A.14}$$

We decompose the group tensor $t_{2\to 4}$ into these normalized transition tensors. With

$$t_{2\to 4}(a_1b_1;a_2b_2c_2d_2) = f_{a_1la_2}f_{lmb_2}f_{mnc_2}f_{nb_1d_2} \tag{A.15}$$

we obtain for the color-singlet channel:

$$t_{2\to 4} = \frac{9}{\sqrt{8}}T_{111} + \frac{9}{4}T_{18_A8_A} + \frac{9}{4}T_{18_S8_S} + \frac{3}{2}\sqrt{\frac{3}{2}}T_{1(27)(27)} \tag{A.16}$$

Next we adress the recoupling problem which now consists of two parts. First we consider the transition 3-reggeon → 4-reggeon (Fig.x). The coefficients are given in Table 1: the symbol (123) indicates that the lines "1", "2", and "3" result from a 2 → 3 transition etc. Next we we look at the four-reggeon final states (Fig.x). For the pairwise interaction in the four reggeon channel we list the coefficients in Table 2. The numbers in the first two columns denote the color quantum numbers ($C'_{12} = C'_{34}$) and ($C_{12} = C_{34}$), resp. For the other columns, (12) denotes the pairwise interaction of the lines "1" etc.

Finally we give the 5×5 matrix which describes the transition from the (12)(34)-coupling scheme to the (13)(24)-coupling scheme. It has the form:

$$\Lambda = \begin{pmatrix}
\frac{1}{8} & -\frac{1}{8} & \frac{1}{8} & \frac{\sqrt{5}}{4} & \frac{3\sqrt{3}}{8}\\
-\frac{1}{\sqrt{8}} & \frac{1}{2} & \frac{1}{2} & 0 & \frac{1}{2}\sqrt{\frac{3}{2}}\\
\frac{1}{\sqrt{8}} & -\frac{1}{2} & \frac{3}{10} & \sqrt{\frac{2}{5}} & \frac{3}{10}\sqrt{\frac{3}{2}}\\
\frac{\sqrt{5}}{4} & 0 & -\sqrt{\frac{2}{5}} & \frac{1}{2} & \frac{1}{4}\sqrt{\frac{3}{5}}\\
\frac{3\sqrt{3}}{8} & \frac{1}{2}\sqrt{\frac{3}{2}} & -\frac{3}{10}\sqrt{\frac{3}{2}} & \frac{1}{4}\sqrt{\frac{3}{5}} & \frac{7}{40}
\end{pmatrix} \tag{A.17}$$

Here the rows refer to the color channels in the (12)(34) scheme, whereas the columns label the color channels of the (13)(24) scheme. The analogous matrix for the transition (12)(34) → (14)(23) is $P\Lambda P$, where $P = diag(1,-1,1,-1,1)$, and the transition (13)(24) → (14)(23) is described by the matrix $\Lambda^T P\Lambda P$. Since Λ is orthogonal, all these transition matrices have this property, and the inverse transformations are equal to the transposed ones. This completes our collection of SU(3) formulae.

Table 1

C	C'_{23}	$C_{12}C_{34}$	(123)	(234)	(134)	(124)
1	8_A	1 1	$-3\sqrt{\frac{3}{8}}$	$-3\sqrt{\frac{3}{8}}$	$3\sqrt{\frac{3}{8}}$	$3\sqrt{\frac{3}{8}}$
	8_A	$8_A\,8_A$	$-\frac{3}{4}\sqrt{3}$	$-\frac{3}{4}\sqrt{3}$	$-\frac{3}{4}\sqrt{3}$	$-\frac{3}{4}\sqrt{3}$
	8_A	$8_S\,8_S$	$-\frac{3}{4}\sqrt{3}$	$-\frac{3}{4}\sqrt{3}$	$\frac{3}{4}\sqrt{3}$	$\frac{3}{4}\sqrt{3}$
	8_A	$10+\bar{10}\;10+\bar{10}$				
	8_A	27 27	$-\frac{3}{\sqrt{8}}$	$-\frac{3}{\sqrt{8}}$	$\frac{3}{\sqrt{8}}$	$\frac{3}{\sqrt{8}}$

Table 2

C	$C'_{12}=C'_{34}$	$C_{12}=C_{34}$	(12)	(34)	(23)	(13)	(24)	(14)
1	1	1	-2	-3				
		8_A			$-\frac{3}{\sqrt{8}}$	$\frac{3}{\sqrt{8}}$	$\frac{3}{\sqrt{8}}$	$-\frac{3}{\sqrt{8}}$
		8_S						
		$10+\bar{10}$						
		27						
1	8_A	1			$-\frac{3}{\sqrt{8}}$	$\frac{3}{\sqrt{8}}$	$\frac{3}{\sqrt{8}}$	$-\frac{3}{\sqrt{8}}$
		8_A	$-\frac{3}{2}$	$-\frac{3}{2}$	$-\frac{3}{4}$	$-\frac{3}{4}$	$-\frac{3}{4}$	$-\frac{3}{4}$
		8_S			$-\frac{3}{4}$	$\frac{3}{4}$	$\frac{3}{4}$	$-\frac{3}{4}$
		$10+\bar{10}$						
		27			$-\sqrt{\frac{3}{8}}$	$-\sqrt{\frac{3}{8}}$	$-\sqrt{\frac{3}{8}}$	$-\sqrt{\frac{3}{8}}$
1	8_S	1						
		8_A			$-\frac{3}{4}$	$\frac{3}{4}$	$\frac{3}{4}$	$-\frac{3}{4}$
		8_S	$-\frac{3}{2}$	$-\frac{3}{2}$	$-\frac{3}{4}$	$-\frac{3}{4}$	$-\frac{3}{4}$	$-\frac{3}{4}$
		$10+\bar{10}$			$-\frac{3}{\sqrt{10}}$	$\frac{3}{\sqrt{10}}$	$\frac{3}{\sqrt{10}}$	$-\frac{3}{\sqrt{10}}$
		27						
1	$10+\bar{10}$	1						
		8_A						
		8_S			$-\frac{3}{\sqrt{10}}$	$\frac{3}{\sqrt{10}}$	$\frac{3}{\sqrt{10}}$	$-\frac{3}{\sqrt{10}}$
		$10+\bar{10}$			$-\frac{3}{2}$	$-\frac{3}{2}$	$-\frac{3}{2}$	$-\frac{3}{2}$
		27			$-\sqrt{\frac{3}{5}}$	$\sqrt{\frac{3}{5}}$	$\sqrt{\frac{3}{5}}$	$-\sqrt{\frac{3}{5}}$
1	27	1						
		8_A			$-\sqrt{\frac{3}{8}}$	$\sqrt{\frac{3}{8}}$	$\sqrt{\frac{3}{8}}$	$-\sqrt{\frac{3}{8}}$
		8_S						
		$10+\bar{10}$			$-\sqrt{\frac{3}{5}}$	$\sqrt{\frac{3}{5}}$	$\sqrt{\frac{3}{5}}$	$-\sqrt{\frac{3}{5}}$
		27	1	1	-2	-2	-2	-2

References

[1] V.N.Gribov and L.N.Lipatov, *Sov.Journ.Nucl.Phys.* **15**, 438 and 675 (1972).

[2] G.Altarelli and G.Parisi, *Nucl.Phys.* **126**, 297(1977).

[3] L.V.Gribov, E.M.Levin, and M.G.Ryskin, *Phys. Rep.* **100**, 1 (1982)

[4] J.Bartels, J.Blümlein, G.Schuler, *Zeitschr. f.Phys.* C **50**, 91 (1991).

[5] J.Kwiecinski, A.D.Martin, W.J.Stirling, and R.G. Roberts, *Phys.Rev.* **D42**, 3645 (1990).

[6] J.Kwiecinsky, A.D.Martin, P.J.Sutton, *Phys.Lett.* **B264**, 199 (1991).

[7] V.T.Kim, M.G.Ryskin, DESY-91-064.

[8] E.A.Kuraev.L.N.Lipatov,V.S.Fadin, *Sov.Phys.JETP* 44,443(1976)

[9] E.A.Kuraev.L.N.Lipatov,V.S.Fadin, *Sov.Phys.JETP* 45,199(1977)

[10] Ya.Ya.Balitzky and L.N.Lipatov, *Sov.J.Nucl.Phys.* **28**, 822(1987)

[11] Ya.Ya.Balitzky, L.N.Lipatov *JETP Letters* **30**, 355(1979).

[12] L.N.Lipatov, *Sov.Phys.JETP* **63**, 904(1986)

[13] A.H.Mueller and H.Navelet,*Nucl.Phys.*B282,727 (1987)

[14] A.H.Mueller, *Nucl.Phys.B*(Proc.Suppl.)18C,125 (1991)

[15] J. Bartels, A.De Roeck, M.Loewe, *Z.Phys.* C54, 635(1992).

[16] J.Bartels, M.Besancon, A.De Roeck, J.Kurzhoefer, in *Proceedings of the HERA Workshop 1992* (eds.W.Buchmüller and G.Ingelman), p.203.

[17] J.Kwiecinski, A.D.Martin, P.J.Sutton, *Phys.Lett* **B287**, 254(1992); *Phys.Rev* **D46**, 921(1992).

[18] W.-K.Tang, *Phys.Lett* **B278**, 363(1991).

[19] J.Bartels, *Phys.Lett.* **B298**, 204(1993).

[20] J.Bartels, DESY 91-074 (unpublished).

[21] V.A.Abramovsky, V.N.Gribov, O.V.Kancheli,*Sov.Journ. Nucl.Phys.* **18**, 595(1973).

[22] H.D.I.Abarbanel, J.B.Bronzan, A.R.White, R.L.Sugar, *Phys.Rep.* **21C** (1975) 119.

[23] J.Bartels, M.Wuesthoff, in preparation.

[24] E.M.Levin, M.G.Ryskin, A.G.Shuvaev, DESY 92-047 and *Nucl.Phys.***B387**, 589(1992).

[25] M.G.Ryskin, *Nucl.Phys.B (Proc.Suppl)***18C**, 162 (1990).

[26] A.J.Macfarlaine,
A.Sudbery, P.H.Weisz, *Comm.Math.Phys.***11**, 77 (1968); *Proc.Royal.Soc.London* **A314**, 217 (1970).

[27] J.Bartels and G.Schuler, DESY 90-167 and to be published in the Proceedings of the ECFA Workshop on LHC, Aachen 1990.

Figure Captions

Fig.1: the $\ln Q^2$-$\ln\frac{1}{x_B}$ plane. The line marks the expected end of perturbative QCD (from [27]).

Fig. 2: (a) six point amplitude in the triple Regge limit; (b) the triple energy discontinuity; (c) reggeon unitarity equation in the partial wave of the elastic scattering amplitude; (d) the AGK cutting rules; (e) the coupling scheme (for angular momentum and color) used in this paper.

Fig.3: the coupled equations for D_2, D_3, and D_4. The summation symbols indicate that the two-body interaction in the lower gluon lines should take place between any two gluons.

Fig.4: diagrammatic illustration of $D_4^{(++)}$ (eq.(3.11): the first two terms (a) denote $D_{(4;2-cut)}$, the last term (b) $D_{4;R}$. Note that in the last term there is no coupling of four gluons to the fermion loop directly.

Fig.5: illustration of the transition vertex. (a) connected and disconnected terms; (b) decomposition of the connected terms following the terms in eq.(3.11); (c) decomposition of the disconnected contributions. In (a) - (c), we have not included the permutations among the lower momenta k_i.

Fig.6: reordering of the four gluon ladders for the calculation of the anomalous dimension.

Fig.7: (a) two ladders below the transition vertex; (b) momentum assignment for a "switch".

Fig.8: singularities in the ν-plane.

Fig.9: illustration of the deep inelastic limit in configuration space (two dimensional impact parameter space).

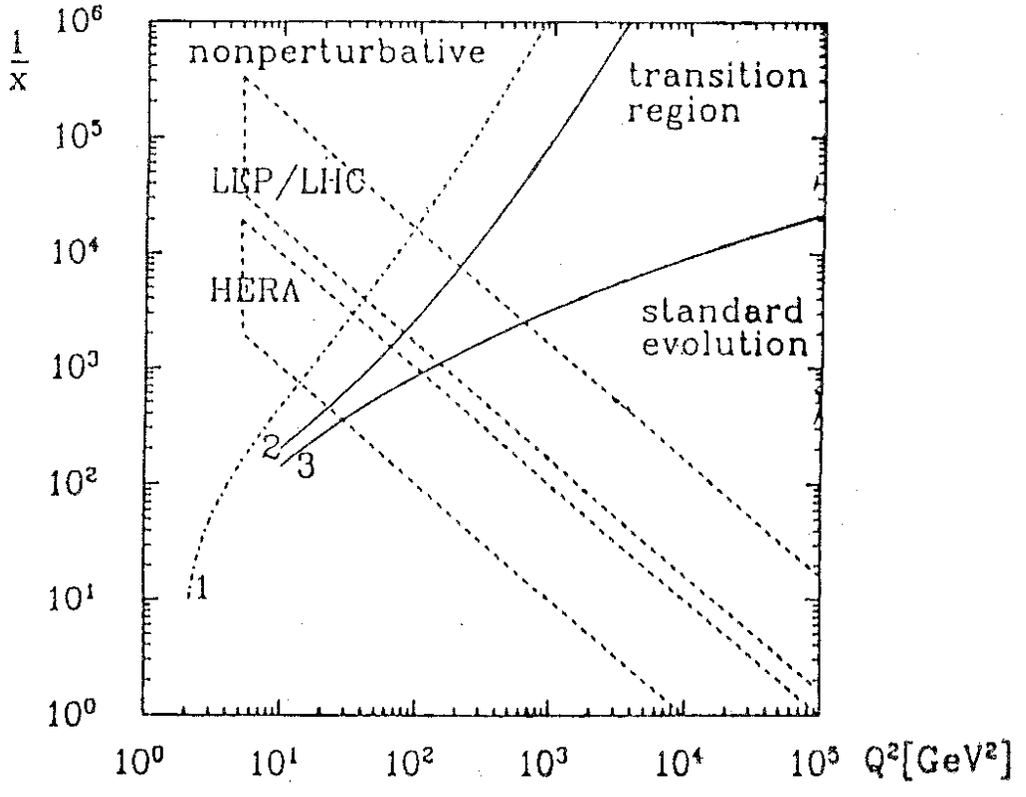
1/x
10^6
10^5
10^4
10^3
10^2
10^1
10^0
nonperturbative
transition region
LEP/LHC
HERA
standard evolution
1
2
3
10^0
10^1
10^2
10^3
10^4
10^5
Q^2[GeV^2]

Fig.1

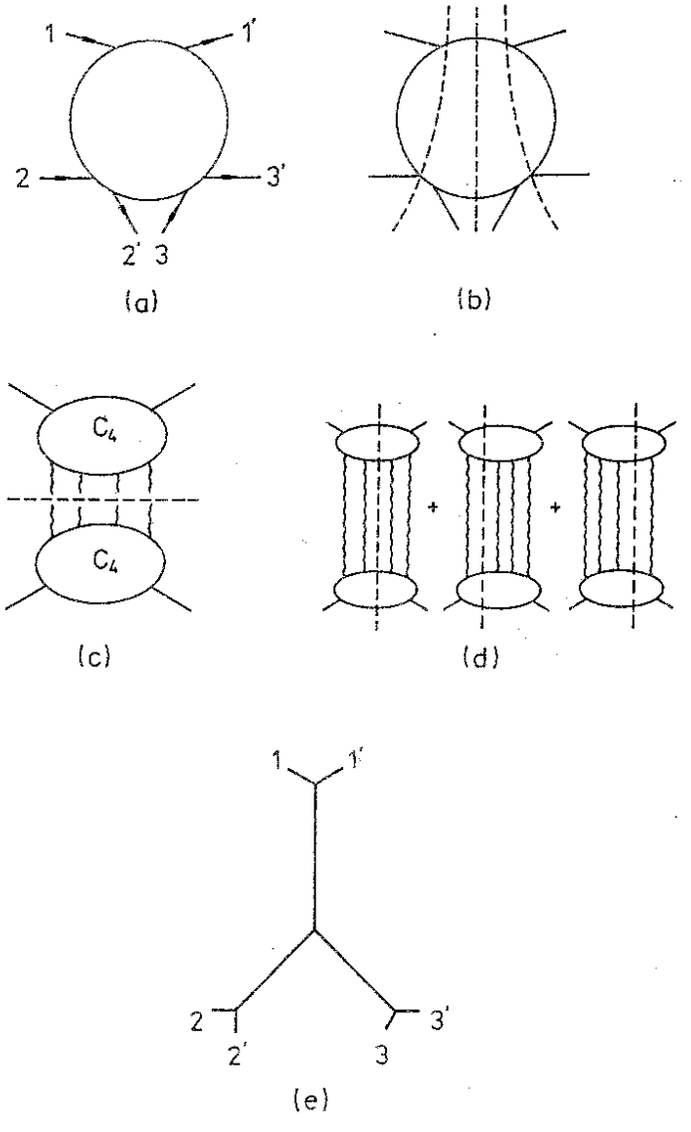
1
1'
2
3'
2' 3
(a)
(b)
C4
C4
(c)
+
+
(d)
1
1'
2
2'
3
3'
(e)

Fig. 2

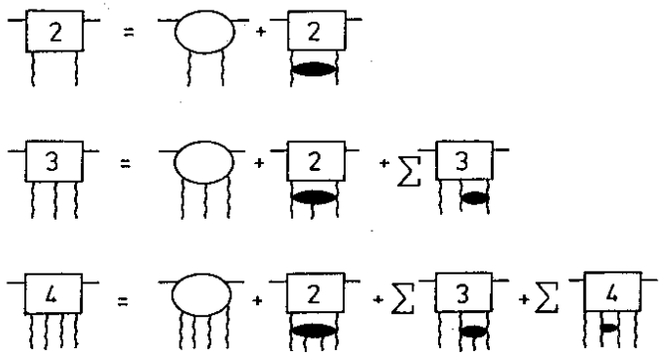

Fig.3

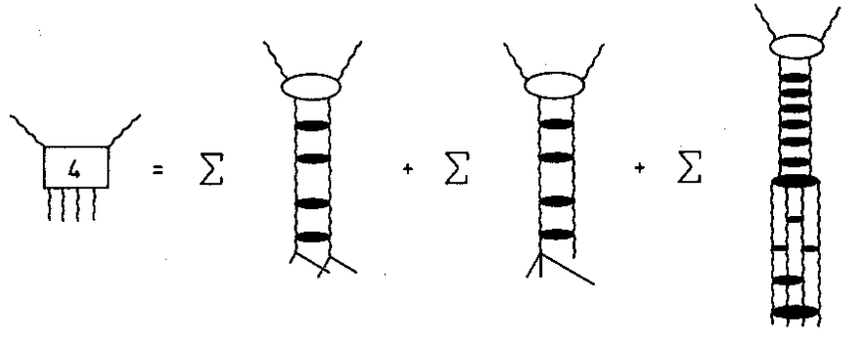

(a) (b)

Fig.4

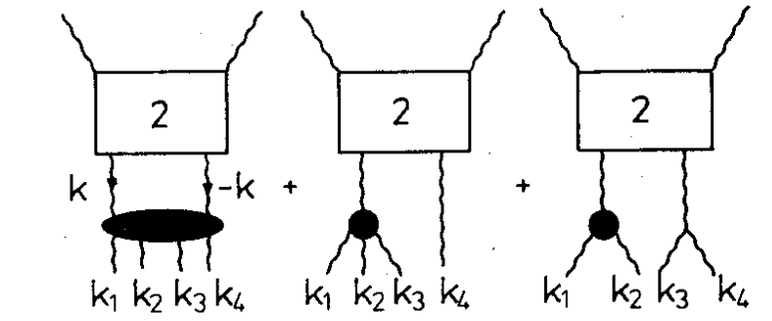

(a)

(b)

(c)

Fig.5

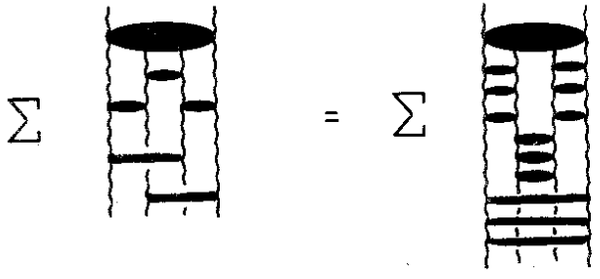

Fig.6

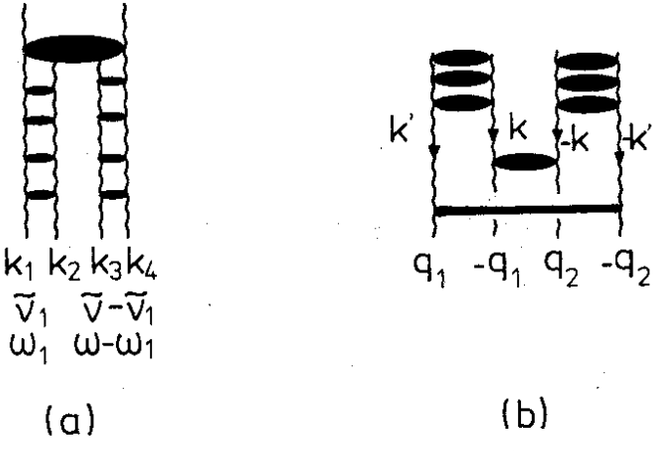

Fig.7

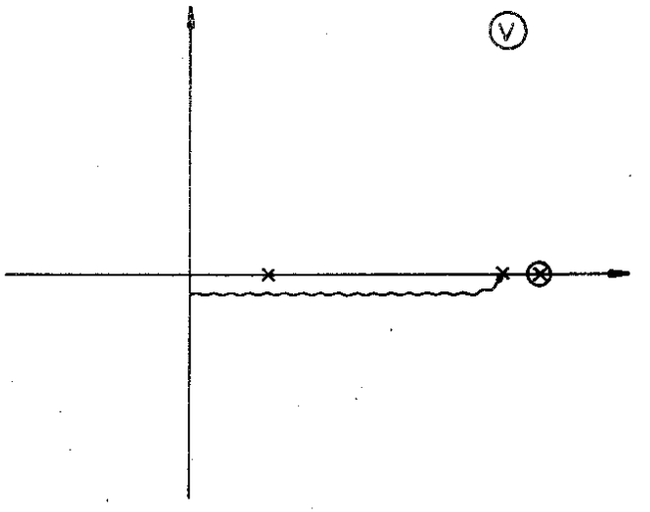

Fig. 8

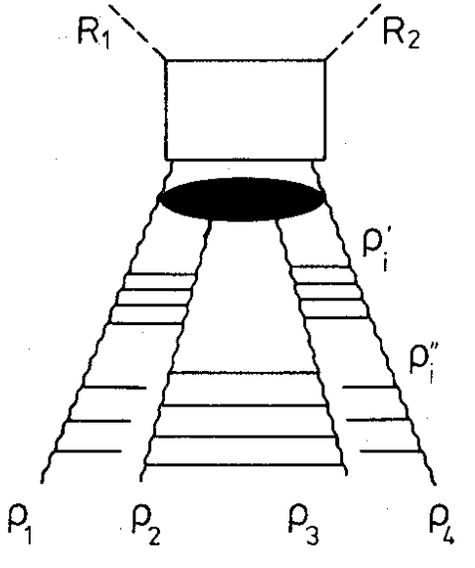

Fig.9